LBL-8254

DESIGN OF A TOKAMAK FUSION REACTOR FIRST WALL ARMOR AGAINST NEUTRAL BEAM IMPINGEMENT

Richard Allen Myers
(M. S. thesis)

December 1977

Prepared for the U. S. Department of Energy
under Contract W-7405-ENG-48

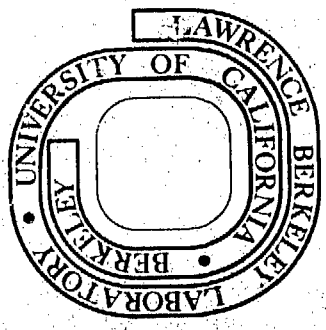

DESIGN OF A TOKAMAK FUSION REACTOR FIRST WALL ARMOR AGAINST NEUTRAL BEAM IMPINGEMENT

Richard Allen Myers
Lawerence Berkeley Laboratory
M.S. Nuclear Engineering Dept.

Protection of the first wall of Tokamak fusion reactors, both for near-term experimental devices, such as TFTR, and fusion power reactors is necessary in view of the high power flux anticipated for neutral beams. The maximum temperatures and thermal stresses are calculated for various design proposals, using both analytical solutions and the TRUMP and SAP IV Computer Codes. Beam parameters, such as pulse time, cycle time, and beam power, are varied. It is found that uncooled plates should be adequate for near-term devices, while cooled protection will be necessary for fusion power reactors. The prevention of fault conditions (a firing of the neutral beam while little or no plasma exists in the vacuum vessel) is shown to be very important to the feasibility of the design.

Graphite and tungsten are selected for analysis because of their desirable characteristics. Graphite allows for higher heat fluxes compared to tungsten for similar pulse times.

Anticipated erosion (due to surface effects) and plasma impurity fraction are estimated. Neutron irradiation damage is also discussed. Neutron irradiation damage (rather than erosion, fatigue, or creep)

is estimated to be the lifetime-limiting factor on the lifetime of the component in fusion power reactors. It is found that the use of tungsten in fusion power reactors, when directly exposed to the plasma, will cause serious plasma impurity problems; graphite should not present such an impurity problem.

TABLE OF CONTENTS

ACKNOWLEDGEMENTS

I would like to sincerely thank Dr. Robert V. Pyle for his advice and encouragement. Similar thanks are due to Rick Steele for his valuable advice,time, and encouragement in getting the computer codes to run. I would also like to thank Drs. Olander and Lieberman for reading the thesis and for their helpful suggestions.

This work was supported by the U. S. Department of Energy.

I. INTRODUCTION

To achieve the extremely high temperatures required by a magnetically-confined fusion reactor plasma, a heating method in addition to ohmic heating will be necessary. Currently, the most promising method appears to be neutral beam heating. A beam of high energy deuterium atoms, almost all of which are in the neutral state, is shot into the plasma, colliding with the plasma ions, causing the plasma temperature to increase. Nearly all of the neutral beam energy will be absorbed by the plasma, but the remaining fraction will impinge upon the first wall of the reactor vessel. This energy flux, even after it has been attenuated by the plasma, may still be high enough to cause excessive melting and/or thermally-induced cracking of the first wall, which would limit the frequency of beam pulses and would require frequent replacement of the first wall. In the event of a "fault" condition, during which the neutral beam is fired while little or no plasma exists in the reactor vessel, the consequences would be even more serious. Finally, since the beam will probably be fired every few hundred seconds, thermal fatigue may be a concern. For the above reasons, protection of the first wall against neutral beam impingement will be necessary.

Unfortunately, more must be considered than the thermal aspects in the design of the armor. The environment in the reactor vessel will be extremely severe. Surface effects, including sputtering, blistering, evaporation, and photo-decomposition, will not only cause erosion of the armor, but will also send armor particles into the plasma; a fusion plasma can endure only a very small percentage of impurities

if it is to achieve ignition and Lawson's Criterion. In addition, neutron irradiation will alter the thermal and mechanical properties of the armor, usually in a degrading manner, and may cause the formation of voids and gas bubbles in the armor, limiting its useful lifetime.

Studies of various design proposals for protection of the first wall have been done in the past.[1-5] Thermal analysis has also been done for calorimeter targets for neutral beams[7,8] and for fusion reactor surfaces in general.[6] However, most of these studies have not considered the effects of erosion, plasma impurities, and neutron irradiation damage, and do not compare the proposal under consideration to other options in a detailed manner. In addition, most of these studies present only a cursory thermal and structural analysis, and in Ref. 2 a two-dimensional, rather than a one-dimensional, thermal analysis should have been employed.

Here, various design options for protection of the first wall of both a near-term device, TFTR, and a fusion power reactor are studied and compared for thermal, structural, and material performance. A brief comparison of materials is made to allow selection of two materials for analysis. The maximum temperatures and stresses reached by the design are calculated using both analytical solutions and the TRUMP and SAP IV computer codes. Erosion rates due to surface effects and the plasma impurity fraction are estimated. Neutron irradiation damage is discussed. Finally, some conclusions are made about the nature of the first wall protection.

It is found that while radiation-cooled armors should be adequate for near-term devices, some form of covective cooling will be necess-

ary for fusion power reactors. The prevention of fault conditions is shown to be extremely important to the feasibility of a design for first wall protection. Graphite and tungsten are chosen as the materials for analysis because of their desirable characteristics. When possible graphite should be employed, because of its lower cost and higher plasma impurity limit. In near-term devices, erosion and neutron irradiation damage should not present themselves as problems. For fusion power reactors, erosion rates will be high, but neutron irradiation damage will probably be the lifetime-limiting factor for the first wall protection. Silicon carbide may turn out to be better than either tungsten or graphite because of its better resistance to neutron irradiation damage. Use of tungsten in fusion power reactors while directly exposed to the plasma, may cause serious plasma impurity problems, while graphite should cause no concern for impurities.

II. DESIGN GOALS

If an armor is to be useful, it should meet as many of the following design goals as possible:

1) Armor lifetime comparable to that of the first wall
2) Low cost
3) Easy fabrication and welding
4) Easy repair and replacement
5) Plasma impurity fraction shouldn't prevent the attainment of ignition or Lawson's Criterion
6) First wall should be protected from damage due to neutral beam strikes.

These goals imply several things about the nature of the first wall protection.

The armor should not be allowed to melt. Melting can be serious both from an erosion viewpoint and from an impurity viewpoint, besides causing damage to the first wall. If melting should occur to even a very small extent during an attenuated beam strike, melting would continue to occur during all successive beam strikes, and a hole may develop in the armor, exposing the first wall. Melting causes very high evaporation rates in many materials, causing rapid erosion rates and possibly high impurity fractions. In addition, evaporated impurities may gradually coat the first wall, making startup difficult even if the plasma and impurities are periodically flushed from the reactor vessel. In addition to limiting the lifetime of the armor, erosion reduces the structural integrity of the armor. The above considerations hold for the fault condition as well, but since this should oc-

cur very rarely, small amounts of melting might turn out to be permissable for a faulted beam strike.

The armor should not be allowed to crack due to thermally-induced short-time rupture. Cracks formed during the attenuated strike will propogate during successive strikes, and eventually small chunks of armor may be flaked off, which is bad from an erosion and impurity viewpoint. Also, the first wall might become exposed if the cracks propogate through the armor. If coolants are used, even very tiny cracks become a cause of concern. Cracking may reduce the effective thermal conductivity of the material. Very small cracks might be allowed during a fault condition if coolants aren't being employed, but since it would be hard to tell what effect these cracks would have on successive attenuated strikes, this cracking should also be avoided.

Fatigue and/or creep may seriously limit the lifetime of the armor, so materials with a long fatigue and creep life should be used.

Materials should be used that do not erode too rapidly due to surface effects. That is, they should have low sputtering and blistering yields. Damage due to neutron irradiation should be minimized, implying the need for materials with low neutron absorption and scattering cross sections. To minimize the effect of impurities in the plasma, low atomic number materials should be used (See Section VII.). The materials should be easily machined and welded, should be available to a large extent as mineral resources in the earth, and should be low cost.

Finally, the geometry of the design should be as simple as possible. Complex geometries not only result in higher stresses generally,

but also increase the cost of the armor.

For some fusion devices, such as TFTR, the weight of the armor may also be a consideration.

III. MATERIALS

Of course there may be no material which is capable of meeting all of the design goals. One should then search for a material which is capable of meeting as many of the above design goals as possible. Desirable characteristics of such materials include:

1) high melting temperature
2) good resistance to thermal shock
3) high thermal diffusvity and emissivity
4) good high temperature performance
5) low evaporation rates
6) high yield, tensile, and compressive strengths
7) long fatigue and creep life
8) low cost
9) easy fabrication and welding
10) large amounts of mineral resources
11) low sputtering and blistering yields against H^+, D^+, T^+, n
12) low atomic number
13) no chemical reactions with hydrogen
14) no corrosion due to common coolants
15) low neutron and photon scattering and absorption cross sections
16) low solubility for hydrogen and helium
17) large amounts of data available on the performance of the material under the conditions of interest.

The best material for the job is likely to be be either a low-Z ceramic or refractory material, such as graphite or silicon carbide,

or a refractory metal, such as tungsten or molybdenum. Many low-Z refractory materials have good resistance to thermal shock, have good high-temperature thermal and mechanical performance, have fair thermal conductivities, and high melting points. They are low cost, are highly available in the earth, and because of their low atomic number they have a relatively high plasma impurity limit. On the other hand, they tend to have high sputtering yields, low yield and fracture strengths, low ductility, many react chemically with hydrogen, and they generally aren't easily fabricated and welded.[9] Refractory metals generally have good thermal shock resistance, high melting points, high thermal conductivities, high strength, fairly long fatigue and creep lives, low sputtering yields, undergo little or no chemical reactions with hydrogen, have good corrosion resistance, and low solubility for hydrogen. However, they have a high cost, are relatively scarce in nature, are not easily fabricated, and have relatively high atomic numbers. Other materials should also be considered that don't fall into either of the above two categories. For example, copper has a very high thermal conductivity. Stainless steel combines the qualities of high strength, low cost, and easy fabrication.

Table I lists several of the candidate materials, their physical and mechanical properties, qualities of interest, and several figures-of merit which provide a rough comparison of the performance of the materials.

The thermal shock parameter is related to the ratio of the tensile strength of the material to the thermal stress developed in the material. It is given by [9]

TABLE I

Properties and figures-of-merit for various materials.

Property	Al_2O_3	BeO	Cr	Cu	C	Mo	Monel	Nb	SiC
$k(W/m/^oK)$	4.1	20.0	91.3	394	180	132	21.7	50	173
$c_p(J/kg/^oK)$	1050	2180	461	386	721	257	423	270	680
ρ (kg/m^3)	3960	3000	7100	8960	2159	10213	8830	8570	680
α $(10^{-6}/^oK)$	9.0	7.5	6.5	17.0	2.6	5.2	13.9	7.02	5.94
$E(GN/m^2)$	345	289	279	117	11.7	329	179	103	414
ν	0.25	0.30	0.26	0.34	0.23	0.33	0.32	0.38	0.26
$T_{melt}(^oK)$	2323	2823	2123	1356	3873	2883	1605	2688	2973
σ tens (MN/m^2)	172	103	414	188	20.7	882	1103	331	172
σ comp (MN/m^2)	276	138			34				1379
Fabrication	Easy	Easy		Easy	Avg.	Hard	Easy	Hard	Avg.
Atomic #	10	6	24	29	6	42	28	41	10
Cost	Low			Low	Low	High	Low	Avg.	Low
Availability	High	Low	Avg.	Avg.	High	Low	Avg.	Avg.	High
S_{D^+} (10 kev)	0.013	0.005		0.065	0.05	0.062		0.008	0.015
S_{He^+}(3 kev)	0.017	0.05		0.25	0.095			0.065	0.001
S_n(14.1 Mev)				0.039	10^{-4}			10^{-3}	10^{-4}
H_2O Corr.	No	No		Little				Little	Litt.
Chem. Sput	No	No		No	Yes				
Emmissivity					0.8				
$k/\rho c(10^{-5}\ \frac{m^2}{sec})$	.998	3.06	2.79	11.3	11.6	5.03	0.58	2.16	8.21
$\alpha E/(1-\nu)$	4.14	3.10	2.45	3.01	.132	2.55	3.66	1.16	3.32
T	1724	6645	15400	24600	27270	45600	6540	14267	8963
F	2.67	2.89	3.22	4.0	5.99	4.82	1.18	2.58	5.12

TABLE I (CONT.)

Property	SS304	Ta	Ti	V	W	B_4C	Si_3N_4	TaC
k(W/m/°K)	19	57	16	31.6	165	26	10.4	34.6
c_p(J/kg/°K)	502.1	142	528	498	135	920	1050	167
ρ (kg/m^3)	7900	16600	4500	6100	19295	2510	3180	14400
α(10^{-6}/°K)	17.3	6.5	8.9	8.3	4.7	4.7	2.6	6.6
E (GN/m^2)	193	186	116	14.7	40.7	448	55.2	283
ν	0.3	0.35	0.33	0.35	0.28	0.21	0.10	0.2
σ_{tens} (MN/m^2)	579	483	873	345	1930	296	109	
σ_{comp} (MN/m^2)						2854	552	
T_{melt} (°K)	1700	3253	1940	2175	3643	2721	2173	4149
Fabrication	Easy			Avg.	Hard	Avg.	Avg.	Avg.
Atomic #	26	73	22	23	74	4.6	10	43
Cost	Low				High	Low	Low	High
Availability	Avg.	Low	High	High	Low	High	High	Low
S_{p+} (10 kev)	0.053	.0042	0.039	0.024	.00089			
S_{He^+} (3 kev)	0.17							
S_n (14.1 Mev)								
H_2O Corros.			No	No		Yes	Little	Little
Chem. Sput.			No			Yes		Yes
Emissivity			0.46		0.3			
k/ρc	.479	2.42	.673	1.04	6.33	.998	.311	1.44
$\alpha E/(1-\nu)$	4.77	1.86	1.54	.188	2.66	2.66	.159	2.33
T	2306	14802	9070	57989	119700	2893	7129	
F	1.22	3.43	1.02	1.84	6.95	1.88	1.11	3.52

$$T = \frac{\sigma_t (1-\nu) k}{\alpha E}$$

where σ_t is the tensile strength, ν is Poisson's ratio, α is the coefficient of thermal expansion, E is Young's modulus, and k is the thermal conductivity. The maximum temperature change ΔT_{max} in an uncooled, semi-infinite plate due to a uniform heat flux q" upon its surface is given by [10]

$$\Delta T_{max} = \frac{2q''}{k} (kt/\pi \rho c)^{\frac{1}{2}} = 2q'' (t/\pi \rho kc)^{\frac{1}{2}}$$

where t is the duration of the heat flux, ρ is the density of the plate, and c is the specific heat of the plate. Assuming that the initial temperature of the plate is 293°K and the plate's melting point must not be exceeded, we arrive at F [7]

$$F = (T_{melt} - 293)(k \rho c)$$

A crude estimate of the maximum thermal stress which develops in such a plate is given by [11]

$$\sigma_{max} = \frac{\alpha E}{(1-\nu)} \Delta T_{max}$$

Thus, a comparison of the strengths of materials may be given by

$$S = \frac{\alpha E}{(1-\nu)}$$

It appears that the two best materials listed are tungsten and graphite; I will use these two materials for calculating the maximum temperatures and stresses attained in the armor design proposals. It may turn out that neither tungsten nor graphite is the optimum material for the job (graphite, for example, may erode too rapidly due to chemical sputtering), but these two materials will provide a good standard of comparison.

IV. DESIGN OPTIONS

Keeping the design geometry as simple as possible is important. As the geometry becomes more complex, the armor would become more difficult to fabricate and the cost would increase. Simple geometries are easier to analyze and generally yield more accurate results. Complex geometries may cause higher stresses due to higher stress concentration factors.

The design geometries considered are listed below and discussed:

IV.A. Free Plate: The main design advantages associated with a simple, free plate are easy fabrication, repair, replacement, and low cost. Analytical solutions for the temperature distributions and thermal stresses in the plate may be easily obtained using certain approximations. Stress concentration factors may be estimated with accuracy. If necessary, the plate could be cooled on the backside (the side not exposed to the heat flux). This backside cooling system wouldn't be exposed to either the neutral beam flux or the plasma flux, giving it a much longer life than the armor plate. The cost of the component would increase, however, with backside cooling.

IV.B. Cubes-on-plate or slotted plate: Because the thermal stesses are generally reduced as the geometry dimensions transverse to the temperature gradient are reduced, two similar modifications of the free plate were considered: 1) small, closely-spaced cubes brazed onto a backing plate[2], not necessarily of the same material as the cubes and 2) a free, slotted plate.[1] While the thermal stresses may be reduced, several disadvantages are introduced using this method. For one thing the cost will undoubtedly increase because of the extra

tasks involved (brazing, slotting, placing the cubes very close together). Secondly, the maximum temperature reached using this type of armor may actually be higher than for the plate. In figure 1 one can see that on a small volume on the edge of the cube, a greater amount of heat flux will be entering the volume than the rest of the surface of the cube, or than the surface of a plate. A two-dimensional temperature analysis will be necessary in this case. (Note that the neutral beam impinges upon the armor at an angle of 45^{o}.) One option, to avoid this unfortunate aspect, is to make the parallelepipeds sucessively larger, as shown in figure 2, but this would increase the cost of the armor further and probably wouldn't be worth the effort anyway. As with the free plate, this design has the option of back-side cooling.

IV.C. Wedged Surface: An armor with a sawtoothed type of surface has the particular purpose of reducing the normal heat flux upon the surface of the material. See figure 3. The normal heat flux varies as the cosine of the angle between the direction of the impinging heat flux and the normal to the surface of the armor. Unfortunately, one can't simply make this angle as large as possible. As the angle of the wedge becomes larger (as the tip becomes sharper) fabrication becomes more difficult. Also, in the small volume near the tip of the wedge, the amount of incoming heat flux is greater than that entering the rest of the wedge, where the heat may diffuse through a relatively larger area. Thus, although the normal heat flux is being reduced, the area that this flux may diffuse through is also being reduced. In addition, the sputtering yield of materials varies as $(\cos\theta)^{-n}$, where θ is the angle between the surface normal and the direction of the striking

particle, (See Section VII.) where n is somewhere between 1 and 2, for $\theta \leq 70^{o}$. This means that for a high value of θ, the sputtering yield will be significantly increased. This type of armor may also be cooled on the backside, and may also be internally cooled. (See fig. 4) Internal cooling, however, will introduce design complexities discussed in Appendix B.

IV.D. Cylindrical Tubes; Internally cooled: This geometry is simple, will achieve much lower temperatures and stresses than uncooled designs, and, since it expected to rapidly approach steady-state, it will allow DC operation of the neutral beam, as is anticipated for fusion power reactors. Rough estimates of the maximum temperatures and stresses can be made using certain approximations. However, to achieve the lower temperatures, the thickness of the tube will have to be very thin ($<$1mm) and this may not be allowable due to sputtering erosion considerations, particularly in view of the fact that the sputtering yield will increase with angle θ. The usual "coolant considerations" in Appendix B must be made. Good contact between the coolant and tube may be assumed using cylindrical geometry.

IV.E. Internally-cooled Rectangular Ducts: (See fig. 5) The principal advantage with this design in comparison to the tube design is that there will be no sputtering yield increase over the exposed surface of the component. However, it may resultin higher temperatures than the tube because 1) the heat flux will not be decreased (due to varying surface normal angle as with the tube) and 2) the shaded area in fig. 5 is slightly more removed from the coolant than the rest of the surface and will reach higher temperatures. Heat transfer will probably be less efficient with rectangular passages, but since the cool-

ant flow will be highly turbulent, this effect shouldn't be significant. This design retains simplicity. The additional coolant considerations must be made.

V. THERMAL ANALYSIS

V.A. Reference Case: To compare the different designs as cocisely as possible, two reference neutral beam conditions were used, one for near-term devices and the other for fusion power reactors. Variations from the reference conditions are given in the second part of this section. The two reference conditions are shown below:

	EXPERIMENTAL REACTOR (TFTR)	POWER REACTOR
MAXIMUM POWER FLUX	10 KW/CM^2	10 KW/CM^2
IMPINGEMENT ANGLE	45^o	45^o
PLASMA ATTENUATION (NORMAL OPERATION)	96%	98%
AMBIENT TEMPERATURE	350^oK	1000^oK
BEAM PULSE TIME	500 msec	STEADY-STATE
CYCLE TIME	300 sec	500 sec
PLASMA POWER FLUX	NEGLIGIBLE	0.3 KW/CM^2

The maximum power flux wasn't increased for the power reactor the neutral beams for such reactors will be spread over a larger area by the time it hits the vessel wall in comparison to TFTR, because of the larger dimensions of the vessel, although the beam will be of greater total power. The larger dimensions of the power reactors will also cause greater attenuation of the beam by the plasma. The vessel wall temperatures in power reactors is expected to be in the range of 500-1000°C. Finally, while the neutral beam for power reactors may not actually be on continuously, a steady-state temperature distribution rapidly develops in cooled designs.

V.B. Maximum Temperatures Attained By Designs:

V.B.1. Free Plate: For a uniform surface heat flux onto a plate of thickness L, assuming that no heat is lost through thermal radiation, and that no heat flows over the back surface, the solution for the one-dimensional temperature distributionin the plate is given by[10]

$$T(x,t) = T_o + \frac{2F_o\sqrt{Kt}}{k} \sum_{n=0}^{\infty} \left\{ \text{ierfc}\left[\frac{(2n+1)L-x}{2\sqrt{Kt}}\right] + \text{ierfc}\left[\frac{(2n+1)L+x}{2\sqrt{Kt}}\right] \right\}$$

where T_o is the initial temperature, F_o is the heat flux, K is the thermal diffusivity, k is the thermal conductivity, t is the duration of the heat flux, and x is the distance from the backface. (The thermal diffusivity is given by $k/\rho c$ where ρ is the density and c is the specific heat.) Since the range of the neutral beam particles is expected to be just a few microns, the neutral beam may be approximated as a surface heat flux. By assuming an adiabatic backface, we've assumed that the plate is thick enough that there is no temperature gradient at the backface. This approach is applicable when $u \geq 1$, where u is defined by

$$u = \frac{L}{2\sqrt{Kt}}$$

Recognizing that the steady-state pulse would melt the uncooled armor, we will use a 0.5 sec pulse time in the above equation and physical properties at 1000°K. We find that the tungsten plate should be greater than or equal to 0.9 cm and the graphite plate should be greater than or equal to 0.6 cm. For convenience, I chose 1 cm as the thickness of the plate.

The maximum temperature in the plate will occur at the exposed surface, i.e. at x=L. Substituting this into the equation for the

temperature distribution, we get

$$\Delta T_{max} = \frac{1.284 F_o \sqrt{Kt}}{k}$$

Using $F_o = F_{max} \cos 45^o = 7.071$ KW/CM^2, t= 0.5 sec, and physical properties at 1000^{o}K, we find that for the tungsten plate $\Delta T_{max} = 3183^o$K, and for the graphite plate $\Delta T_{max} = 3620^o$K. (See Appendix C for thermal and mechanical properties vs. temperature for tungsten and graphite.) Note that, although these temperatures are quite high, vaporization should not occur to a large degree because the neutral beam will be on for only 500 msec at the most. (While 1000^{o}K isn't the average temperature, properties at that temperature seem to be a good estimate of temperature-averaged properties.) The maximum temperature attained during attenuated pulses will, of course be much less than those found above.

However, to be accurate we must consider the effects of thermal radiation and successive attenuated pulses followed by a fault condition. To calculate the temperatures approached by the plate after a series of pulses or cycles, the TRUMP Thermal Analysis Computer Code was used. (See Appendix A.) The maximum temperatures reached by the plate during the beam pulse and the temperatures reached at the end of the cycle are shown in figures 6a and 6b, graphed vs. the number of beam cycles. Then, TRUMP was used to calculate the temperature change due to an unattenuated strike on the armor, which was found to be 3127^{o}K for tungsten and 3507^{o}K for graphite. One would expect melting if a fault condition should occur following a series of attenuated pulses, in view of the melting point of tungsten (3643^{o}K), and the sublimation point of graphite (3873^{o}K).

V.B.2. Backside-cooled, Free Plate: If the reference case parameters are used, backside cooling will be necessary for a free plate in "experimental" reactors. The maximum temperature reached by the plate should be substantially reduced and thermal cycling analysis will not be necessary because the plate temperatures will rapidly approach the coolant temperature after the beam pulse has ended. However, the beam heat flux will not penetrate substantially into a 1 cm plate during the pulse of 0.5 sec. For longer pulse times the surface temperature will have risen to such an extent as to make backside cooling ineffective. Thus, the thickness of the plate will have to be reduced.

The temperature distribution in a plate exposed to a constant, uniform heat flux, F_o, at x=L, while the back face is kept at the initial temperature, T_o, is given by [10]

$$T(x,t) = T_o + \frac{2F\sqrt{\kappa t}}{k} \sum_{n=0}^{\infty} (-1)^n \left\{ \text{ierfc}\frac{(2n+1)L-x}{2\sqrt{\kappa t}} - \text{ierfc}\frac{(2n+1)L+x}{2\sqrt{\kappa t}} \right\}$$

Again, we would expect T_{max} to occur at x=L. Thus,

$$\Delta T_{max} = \frac{F_o L}{k} - \frac{8F_o L}{k\pi^2} \sum_{n=0}^{\infty} \frac{e^{-(2n+1)^2\pi^2 t/4L^2}}{(2n+1)}$$

$$= \frac{F_o L}{k} \left(1 - 0.81e^{-\kappa\pi^2 t/4L^2} \right)$$

One can easily see that as $t \to \infty$, $\Delta T_{max} \to \frac{F_o L}{k}$. Using various thicknesses and temperature-averaged properties, ΔT_{max} is listed in Table II. Also shown are TRUMP calculations using a heat transfer coefficient between the backface and the coolant of 1.0×10^5 W/M^2-^oK, and a constant coolant temperature of 350^oK, rather than a constant backface temperature. These TRUMP conditions should be much more representative of reality and should be used in preference to the

TABLE II

T_{max} For Various Plate Thicknesses With Back Face Cooled

Thickness	Tungsten	Trump	Graphite	Trump
5 mm	3536 ^{o}K	3000	7043	3645
2 mm	1296	2000	2817	3150
1 mm	556	1330	1204	2010

F= 7.071 Kw/cm^2

$t \rightarrow \infty$

TABLE III

T_{max} Vs. Thickness For Backside Cooled Plates, Using Different Values of the Heat Transfer Coefficient

h(W/m^2/^{o}K)→	1.5 X 10^5		2.0 X 10^5	
Thickness	Tungsten	Graphite	Tungsten	Graphite
2 mm	1730	3050	1531	2699
1 mm	1060	1740	930	1550

F= 7.071 Kw/cm^2

$t \rightarrow \infty$

analytical solution. Increasing the heat transfer coefficient, by increasing the coolant velocity or by employing swirl tubes, would decrease ΔT_{max}. For heat transfer coefficients of 1.5 and 2.0 X 10^5 W/M^2-^oK, TRUMP calculated the maximum temperatures shown in Table III.

Backside cooling substantially reduces the temperatures in the free plate and will prevent melting of tungsten and graphite plates for a steady-state reference heat flux. Maximum allowable heat fluxes will be reviewed in the third part of this section.

V.B.3. Cubes-on-plate or Slotted Plate: There is really no need to perform a thermal analysis for the uncooled design for the TFTR or power reactor reference conditions since we already know by the free plate analysis that melting will occur. Backside cooling will be reviewed here.

For the reference condition, the thickness of the cubes or plate is the main parameter of interest. It was assumed that the cubes were placed close enough together (or that the plate was slotted finely enough) that only the top tenth of the thickness of one edge of the cube was exposed to additional heat flux. Using a steady-state reference heat flux upon the armor, h= 1.0 X 10^5 W/M^2-^oK, and a constant coolant temperature of 350^oK, TRUMP calculated the ΔT_{max} for free plates of similar thicknesses to 10-20% less than for this type of armor. Indeed, melting would still occur for the tungsten cube at a thickness of 5 mm, but not at 2 mm. The temperature of the graphite armor would just exceed the sublimation point at a thickness of 2mm. In spite of these higher temperatures, this design still be considered useful if the thermal stresses are substantially reduced.

V.B.4. Wedged Surface: The maximum temperature for this design should be reached in the tip of the wedge. The main variations involved with this design are the angle of the wedged surface and the material combinations. For example, a tungsten tip might be brazed onto a copper base. The maximum temperatures in the tip and in the base material, if the base material is composed of a different material, are shown in Table IV, for the unattenuated reference heat flux and a 0.5 sec pulse. The height of the wedge was varied between 15-35 cm with no significant change in these temperatures. Note that the increase in angle causes an increase in T_{max}. Also, while copper significantly reduced T_{max}, it will still melt because of copper's low melting point. The temperatures are probably too high for a braze anyway.

These temperatures are significantly high to abandon this design. This design is also more difficult to fabricate than the previously-discussed designs. Backside-cooling was not considered; in view of these high temperatures, the height of the wedge would have to be reduced by an impractical degree.

V.B.5. Internally-cooled Wedge: Many parameters need to varied with internal cooling. See Appendix B. However, there are a few limits that can be imposed in the design process. First, in consideration of the erosion calculations in Appendix D, the thickness of the wedge wall should be limited to greater than or equal to 0.3 mm. Since W appears to have the lowest sputtering yields of all materials, this limit should apply to other materials as well. Secondly, the coolant velocity should be less than or equal to 90 M/SEC. While increasing the heat transfer coefficient further (by increasing the coolant velocity further) would result in even lower temperatures, it would also

TABLE IV

Maximum Temperatures In Wedge Tip and Base, For Various Wedge Angles and Material Combinations.

	Angle		
Materials	45^{o}	60^{o}	80^{o}
W only	3800	4200	5000
W on Cu	1900 (1900)	2200 (2200)	2600 (2600)
C only	4300	5000	
C on SiC	4300 (4300)	5000 (5000)	

T is in ^{o}K.

Tip temperature is listed first; T_{max} for the base is listed in parentheses.

increase the pressure drop and the required pumping work by an even greater degree. The probability of burnout also increases with pressure drop, but since high pressure is being used this consideration may not be significant. Very high velocities might cause high stresses in the tube wall, too. As mentioned, to prevent burnout I chose the pressure of the water coolant to be in the range of 1500-2000 psi. This not only increases the saturation temperature, but increases the heat transfer coefficient as well. However, it also increases the stresses in the wedge wall. The length of the coolant passages for calculation purposes was chosen to be 1 m. Neutral beam diameters hitting the first wall aren't expected to exceed this. The equivalent diameter of the coolant passage is a variable, but diameters in the range of 8-12 mm was generally used in the calculations. While allowing a smaller diameter increases the heat transfer coefficient, it decreases the mass flow rate. Larger diameters increase the mass flow rate, but decrease the design's structural integrity because of an increase in the hoop stress.

The heat transfer coefficient, boiling crisis conditions, and general coolant considerations are discussed in Appendix B.

For the unattenuated power reactor reference conditions and various wedge and coolant characteristics, the maximum temperatures in the tip and the base of the wedge were substantially reduced (roughly by a factor of 1.5), but the temperatures for a circular tube were reduced by an even greater degree for similar conditions and heat transfer coefficients (See below.), so the wedged surface design was totally abandoned.

V.B.6. Cylindrical Tube: Because of the complex nature of the analyt-

ical solution that would be found if Fourier's Equation and the appropriate boundary conditions were solved for, I chose to use only TRUMP to carry out the thermal analysis for the tube design. For various tube and coolant conditions, the unattenuated power reactor reference case produced the maximum temperatures in the tube shown in Table V. In several of the cases however, the burnout heat flux came very close to being exceeded. For example, in the case of V= 30 M/SEC and a tube thickness of 0.8 mm and 1.0 mm, the burnout heat flux was calculated to be slightly greater than 7.0 KW/CM^2 for tungsten and slightly less than 7.0 KW/CM^2 for graphite. Burnout was not achieved in any of the V= 60 M/SEC or V= 90 M/SEC cases.

T_{max} is lowest for this design for all of the designs thus far discussed. It was also found that the temperature difference across the thickness probably won't cause yielding of the tube, when added to the pressure stress. Finally, the increase in the mass flow due to an increase in the diameter apparently had an insignificant effect on the maximum temperature reached by the tube. Maximum allowable fluxes will be reviewed in the third part of this section.

V.B.7. Internally-cooled Rectangular Ducts: As predicted the maximum temperature for this design occurs in the upper corner of the parallelepiped. T_{max} was again calculated by TRUMP for various duct and coolant parameters. The results are shown in Table VI. Although the maximum temperatures attained in each case here are slightly higher than for the tube under similar conditions, the difference is not overwhelming and this design should remain a viable alternative at this point.

TABLE V

T_{max} For Tubes With Various Coolant and Tube Characteristics

(Unattenuated, Steady-State Heat Flux)

Graphite — Velocity (m/sec)

Thickness	30	60	90
0.3 mm	1380	1150	980
0.5	1680	1400	1272
0.8	2652 *	2210	1685
1.0	2800 *	2400	2050

8 mm D 12 mm

p= 2000 psi

* Burnout heat flux exceeded or approximated.

Tungsten — Velocity (m/sec)

Thickness	30	60	90
0.3 mm	1074	935	880
0.5	1220	1135	1005
0.8	1450	1310	1191
1.0	1860 *	1500	1351

TABLE VI

T_{max} For Cooled Rectangular Ducts

Graphite	Velocity (m/sec)		
	30	60	90
Thickness			
0.21 mm	1530	1184	1070
0.45	1851	1453	1295
0.75	2220 *	1798	1625

D_e = 9.2 mm

p= 2000 psi

* Burnout heat flux exceeded or approximated.

Tungsten	Velocity (m/sec)		
	30	60	90
Thickness			
0.21 mm	1300	1106	1000
0.45	1491	1290	1147
0.75	1625 *	1360	1229

V.C. Variations From The Reference Case:

V.C.1. Free Plate: Since the uncooled plate will melt under an unattenuated beam strike following a series of attenuated strikes, it is necessary to find conditions under which melting won't occur. These conditions may include a decreased heat flux, a decreased pulse time, or both.

The equation for ΔT_{max} in the semi-infinite plate is given by

$$\Delta T_{max} = \frac{1.1284 F_o \sqrt{\kappa t}}{k}$$

Setting $\Delta T_{max} = T_{melt} - T_o$, we can get an equation for allowable values of the heat flux and the pulse time:

$$F_o \sqrt{t} = \frac{(T_{melt} - T_o)\, k}{1.1284 \sqrt{\kappa}} = \frac{(T_{melt} - T_o)}{1.1284} \sqrt{k \rho c}$$

Thus, we may graph F_{omax} vs. the beam pulse time for various values of the initial temperature. This is shown in figures 7a and 7b. It would appear that the maximum allowable flux would be between 5.5 and 6.5 KW/CM^2 for tungsten and 6.0 to 7.0 KW/CM^2 for graphite. Using figures 6a and 6b, we can see that for tungsten the asymptotic temperature at the end of the cycle for 0.24 KW/CM^2 (6.0 X 0.04) is about 650°K, and for 6.0 KW/CM^2 the temperature rise is about 3000°K for a 0.5 sec pulse time. Thus, at 6.0 KW/CM^2, the melting point for tungsten would just be exceeded. At 6.5 KW/CM^2, the sublimation point for graphite would not be exceeded.

V.C.2. Cube-on-plate: For the uncooled cube or waffle type of design, the effect will be similar to that above, but the allowable heat flux will be lower. Since the maximum temperatures reached by the cube

armor is roughly 10-20% higher than for the plate, it seems reasonable to assume that the maximum allowable heat flux for a particular pulse time would be roughly 83-91% (1/1.2-1/1.1) of F_{omax} for the plate. For example, a heat flux of 5.0 KW/CM^2 was first used as an attenuated beam to get a temperature at the end of the cycle after many cycles for a tungsten cube. This turned out to be about 630^oK. The unattenuated strike caused a temperature increase of 2850^oK. Thus melting would be avoided at 5.0 KW/CM^2 for a tungsten cube. The maximum temperature increase was 3350^oK for 6.0 KW/CM^2.

It would seem that lowering the heat flux and increasing the pulse time would be very beneficial to the performance of the armor.

V.C.3. Backside-cooled, Free Plate: From the erosion calculations in Appendix D, a 1 mm thick plate should be adequately thick. I increased the heat flux on tungsten and graphite plates to find the maximum allowable heat flux. Again, $T_{cool} = 350^oK$ and $h = 1.5 \times 10^5$ W/M^2-^oK, F_{max} on the tungsten plate was found to be greater than 13 KW/CM^2 for W and graphite, but burnout would probably occur before this heat flux was allowed.

V.C.4. Tube: The main parameters varied here were the heat flux and the pressure of the coolant; the heat flux was varied to determine its maximum allowable value before melting or burnout was achieved; the pressure was varied to determine how low the pressure could be taken and still have reasonable heat transfer and not exceed the burnout heat flux. The velocity of the coolant was chosen to be 90 M/SEC for these calculations. The various combinations of pressure and heat flux are shown below in Table VII. It would seem that if neutral beam

TABLE VII

Effect of Heat Flux and Pressure on T_{max} and q_c'' for Tungsten Tubes

F $(\frac{Kw}{cm^2})$	T_{max} (°K)	q_c'' for p= 750 psi	1400	2000
8.48	1000	$\Delta p > 750$	15.4	19.1
10.61	1230	$\Delta p > 750$	14.3	17.6
12.73	1473	$\Delta p > 750$	13.9	15.4
14.85	1760	$\Delta p > 750$	13.4	13.9

Thickness= 0.3 mm

Velocity= 90 m/sec

power fluxes are going to exceed 7 KW/CM^2, high pressure coolant will be necessary to avoid burnout. Also, melting is not the primary concern when dealing with high velocity coolants at high heat fluxes. Fluxes will be limited by either burnout or thermal stress. Finally, very high velocity coolant will be needed if fault conditions are allowed to occur to prevent burnout, melting, and cracking due to thermal stress.

The pressure and heat flux effects would be similar for an internally-cooled, rectangular duct.

V.D. Summary:

Uncooled plates are seen to be adequate for heat fluxes slightly lower than the reference heat flux and a pulse time of 0.5 sec. For the cube or slotted plate designs, the heat flux must be lowered even further, by about 10-20%, to avoid melting during fault conditions. Erosion of these uncooled plates is not a major concern, considering the expected thicknesses of these plates and the erosion calculations in Appendix D.

Backside cooling drastically reduces the temperature of the plates but a thickness of less than 2 mm must be allowed for. Erosion may become a concern if the cooled armor's lifetime must be more than about ten years, but neutron irradiation damage will probably not allow that anyway.

A wedged surface because of its higher temperatures and increased erosion due to its angle to incident particles, was rejected as a design proposal. Internal cooling was not adequate to substantially reduce the temperatures to a level that is competitive with other design proposals.

Internally-cooled tubes are seen to be adequate not only for the experimental and power reactor reference cases, but also for increased heat fluxes if high velocity coolant is allowed. Erosion, however, remains a major concern.

The internally-cooled rectangular ducts reach slightly higher temperatures than the tubes, but the difference is not overwhelming. This design remains in consideration because of its lower erosion rate than the tube.

If heat fluxes may be lowered and pulse times increased, the performance of the armor will be better particularly for the uncooled armors. Or, if the pulse time were decreased and the heat flux increased, the same would be true. (For near term experimental machines the energy confinement times will be on the order of 0.1-1.0 sec. For fusion power reactors the energy confinement time will be on the order of several seconds. For ignition types of Tokamaks, ideally, the neutral beam pulse time should be at least as great as the energy confinement time.[54])

VI. THERMAL STRESS

A. Introduction

Thermal stresses may arise in a heated body either because of a nonuniform temperature distribution, external constraints, or both. Although we will need to consider the effects of external constraints, our chief concern here is for stresses due to temperature gradients in the first wall armour.

If a body is heated uniformly each differential volume of the material will expand by the same amount and no stresses will arise if the body's boundaries are not restrained. However, if the body is heated nonuniformly the differential volumes will not expand evenly. Each will expand according to its own temperature rise. Since the body must remain continuous (till it fractures), internal constraints are created, because each of the differential volumes will be restraining the distortions of the surrounding volumes, and stresses result. Stresses do not result, however, in the case of temperature distributions which are linear in rectangular Cartesian coordinates (See Ref. 11, pg. 272-273). Generally speaking, the larger the temperature gradient, the larger the thermal stresses will be.[11]

For all of the designs considered, a non-linear temperature gradient exists; we should expect some degree of thermal stress and strain. To calculate the thermal stresses where an analytical solution was not available SAP4 was used. SAP4 is a structural analysis program for linear, elastic materials.[20] The analytical solutions that I used were also based on linear, elastic theory.

(for a brief discussion of SAP4, linear vs nonlinear theory, and static vs dynamic analysis, see App. A.)

VI. B. STRESSES ATTAINED IN DESIGNS

VI. B.1. Free Plate:

For a plate, free of external fractions, unifo: mly heated on one surface, with the other surface insulated, the thermal stress distribution is given by

$$\dot{6}_{xx} = 6_{yy} = \frac{1}{1-\nu}\left\{ - \alpha E T + \frac{\alpha E}{2h}\int_{-h}^{h} T\, dz + \frac{3z\alpha E}{2h^{\partial}} \int_{-h}^{h} T\, z\, d\, z \right.$$

$$= \frac{F_o h \alpha F}{K(1-\nu)} \left\{ \frac{1}{4}\left[\frac{1}{3} - \frac{z}{h}^{2}\right] + \frac{4}{\pi^2} \sum_{n=1}^{\infty} \frac{(-1)^n}{n^2} e^{-\frac{n^2\pi^2 Kt}{4h^2}} \cos\frac{n\pi(Zth)}{2h} \right.$$

$$\left. \left. - \frac{48\, z}{h\pi^4} \sum_{n=1,3,5}^{\infty} \frac{e^{-\frac{n^2\, 2_{Kt}}{4h^2}}}{h^4} \right\} \right.$$

where α is the thermal coefficient of expansion, E is Young's modules, ν is Poisson's ratio, z is the diatance measured from the center of the plate, and 2h is the thickness of the plate. (The plate is heated at the surface where z = th.) All other parameters have been previously defined. In our case, a conservative assumption is to have the entire plate heated at the maximum heat flux. From the previous chapter we found the maximum allowable heat flux for

a 0.5 sec pulse time to be about 5.5 $\frac{KW}{cm^2}$ for a tungsten plate and about 6.5 $\frac{KW}{cm^2}$ for graphite. Using these heat fluxes and a 0.5 sec pulse time, and assuming average physical and mechanical properties, the stress distributions shown in fig. 8a, b for the unattenuated heat fluxes were calculated. (Note that I've assumed that the temperature gradients are greatest at the end of the pulse, TRUMP calculations show this to be the case.)

Compared with the U.T.S. of tungsten and graphite, it can be seen that probably yielding and possiblity fracture will occur for the unattenuated pulse. The attenuated pulse will not caused yielding. If yielding is not allowed to occur then the flux will have to be reduced even further, to about 2.5 - 3.0 $\frac{KW}{cm^2}$ for tungsten and 3.5 - 4.0 $\frac{KW}{cm^2}$ for graphite. Note that the maximum compressive stress, while several times larger than the tensile stress maximum, may be allowed to be larger than the U.T.S., because the compressive strengths of most materials is much more than their tensile strengths. I could not find compressive strengths for tungsten and assumed, conservatively, that its tensile strength equals its compressive strength.

VI. B. 2. Cube design:

It would not be a good assumption to assume that a free plate analysis is applicable to this design because for one thing, the dimensions of the cube on slotted place are too small and secondly the cube (or that part of the slotted plate which lies above its backing plate) will be essentially under restraint by the backing plate.

I used just one type of restraint, however, because in Ref. 3, it was found that variation of the restraint conditions has little effect on the stress distribution, particularly in the hotter regions, where we are interested. I used restraint at a single point (in the center of the plane connecting the cube to the backing plate) in all three directions and restrained all modes in a direction transverse to the temperature gradient, I also used a one dimensional temperature distribution, using the maximum temperature for an entire layer as the temperature at a certin height of the cube.

For the allowable heat fluxes I found the temperature distribution from TRUMP for the unattenuated case, and put these values in SAP4 to find the stresses. I did the same for the attenuated case. It can be seen See Fig. IX that the stresses are lower than those found for the free path for the attenuated flux. (By decreasing the width of the cube or slotted plate, the stresses should be reduced even further.) However, yielding will still occur, and possibly fracture, for the unattenuated flux, if the SAP results are to be belived at such high temperature. For the unattenuated flux, though, linear, elastic theory would break down, making both SAP4 and the analytical solution for the free plate quantitatively incorrect. This is why the cube results actually show higher stresses than the free plate results for the unattenuated flux.

VI. B. 3. Backside - cooled plate

From the analytical expression for the temperature distribution for a plate, which is exposed to a uniform heat flux and kept at the initial temperature on the opposite surface, one can see that as $t \to \infty$, and that the stress has passed through a maximum at a previous

time. Schivell and Grave have found that the maximum dimensionless stress, $\frac{\pi^2 K(1-\nu)\sigma_{max}}{8LFE\alpha}$, occurs at the exposed surface of the plate at a time $t = 0.1\tau$ where τ is a time constant, $\tau = \frac{4L^2}{\pi^2 K}$. This maximum stress is compressive and has a value, in dimensionless terms, of -0.126. The maximum tensile stress also occures at $t = 0.1$, its value is about + 0.042. For tungsten and graphite plates less than 5mm thick it is less than 0.5 sec, which means that the maximum stress would occur before the end of the 500 msec neutral beam pulse. Replacing the dimensionless stress with actual stress values and physical properties, we can find the maximum stresses which would occur for attenuated and unattenuated beat fluxes on various thickness plates. These stresses are shown below Note that the attenuated flux

TABLE IX

EFFECT ON BACKSIDE-COOLED PLATE THICKNESS ON MAXIMUM STRESS

		TUNGSTEN			GRAPHITE		
Thickness [mm]		5mm	2	1	5	2	1
ATTEN.	$\sigma_{tens.}$	7.72	3.09	1.54	0.102	0.042	0.021
Flux	σ_{comp}	23.2	9.28	4.64	0.314	0.126	0.063
UNATTEN.	σ_{tens}	297	113	47.7	13.1	5.25	2.62
Flux	σ_{comp}	891	340	143	39.4	15.8	7.87

causes no yielding or fracture, while the attenuated flux will cause yielding or fracture for plates thicker than about three or

four mm for tungsten. Plates of graphite even 5mm thick wouldn't be expected to crack under the unattenuated flux. While the more realistic example of using a heat transfer coefficient at the back face would yield higher temperatures, the temperature gradients aren't expected to be any greater than for a constant back-face temperature; consequently, the stresses aren't expected to be any greater.

The stresses could be reduced even further if a cube-type of design was used, but since the stresses in the backside-cooled plates are sufficiently low, there is really no need to consider it. Presumably, the degreee of reduction would be on the same order as that produced by the uncooled cube-type armour, i.e. about a factor of two or three.

VI. B. 4. Tube:

As mentioned previously steady state temperature were approached very rapidly by all the tubes tested; most of the heat flow is in the radial direction, although the azimuthal temperature gradient can't be totally ignored.

For a thin-walled tube with a temperature difference across the wall, the thermal hoop stress is given by $\frac{\alpha E}{2(1-\nu)}\Delta Tw$ where ΔTw is the temperature difference $(T_o - T_i)$, at distances far from the end of the tube. At distances closer to the ends the hoop stress due to a temperature gradient is increased by a fractor of 1.25. The pressure-induced hoop stress is given by $\frac{\rho D}{2T}$ for a thin-walled tube, where ρ is the pressure, D is the average diameter of the tube and t is the thickness of the tube wall. Thus we would expect the maximum stress in the tube to be given by $\frac{\rho D}{2t} + 1.25\ \frac{\alpha E}{2(1-\nu)}\ \Delta Tw_{max}$

The maximum temperature difference across the wall will occur at the zenith of the tube, at the point which is exposed to the maximum heat flux. Since, at steady-state, TRUMP showed the temperature gradient to be almost linear in terms of r, the radial direction, ΔT_{max} should be given roughly by $(F_{max}\ t)/K$. On can see that the temperature difference across the wall should decrease as the thickness of the wall is decreased. In the TABLE below ΔT_{max} is listed for various - thickness graphite and tungsten tubes using average physical properties. Also listed is ΔT_{max} for tubes calculated by TRUMP using the coolant velocities shown.

TABLE X

ΔT_{max} across the thickness of tubes

TUNGSTEN THICKNESS (mm)	$\frac{F_{max}\ t}{K}$	TRUMP $\Delta T_{wall\ max}$ V = 30 m/sec	TRUMP $\Delta T_{wall\ max}$ V = 90 m/sec	$\frac{MN}{m^2}$ σ_{max}	$\frac{MN}{m^2}$ σ_{max}
0.3	153	190	175	$\geq$389	$\geq$482
0.5	256	325	295	$\geq$479	$\geq$577
0.8	467	580	630	$\geq$787	$\geq$1020
1.0	609	645	640	$\geq$894	$\geq$939
GRAPHITE					
0.3	162	275	285	$\frac{\rho D}{2t}$ > 10,000 psi	
0.5	289	500	555		
0.8	622	900	935		
1.0	946	1340	1320		

Several things may quickly be noticed from the above table 1) ΔT_{max} as calculated by TRUMP, doesn't vary much with coolant velocity. 2) ΔT_{max} calculated by TRUMP is higher than that calculated by the simpler method. Physical properties will make some difference, but one wouldn't expect the difference to be quite as large as indicated. 3) I didn't calculate the total stresses for graphite, because in each case the yield stress was exceeded. Indeed, even for a pressure of about 750 psi the yield stress would be exceeded for tubes of thickness greater than about 0.6 mm.

We may therefore conclude that graphite should not be used for the tube design and that tungsten tubes of thickness 0.5 mm shall not be considered for the reference power reactor conditions. In addition, it can be seen that increasing the heat flux beyond the reference flux will increase the thermal stress. Considering that the maximum allowable stress is, from App. C, about 68×10^7, we can see that the maximum allowable flux is roughly $7 \times \frac{68 \times 10^7}{48 \times 10^7} = 10 \frac{KW}{cm^2}$ if the TRUMP temperature difference is used, F_{max} is about 8.2 kw/cm^2 for a 0.5 mm thickness tube. For a 0.3 mm thick tube, the maximum allowed flux is $7 \times \frac{68}{48} = 10 \frac{KW}{cm^2}$. Remember that this doesn't consider the stresses created due to the azimuthal temperature gradient either, but since the azimuthal gradient is roughly 10% of the radial gradient, one wouldn't expect the total stress to be more than 1.1 times that shown in the previous table.

A simple analysis using constant properties shows (See fig. X) that the optimum thickness for a tungsten tube is about 0.28 mm, if the stress is to be kept minimum. Also shown is the yield stress at function of tube thickness. (Actually this is yield stress as a

function of temperature; the temperature of the tube increases with increasing thickness.) This shows that the maximum allowable thickness for a tungsten tube is about 0.6 mm in terms of stress considerations for the reference heat flux.

Copper, while being a very good conductor, could not be used because its yield stress is very low.

Internally-Cooled "Plate": Stress considerations for the internally-cooled plate would be identical to that for the tube, for the most part. However, the stresses will be even higher than the tube because of the higher temperatures occuring in the corner of the rectangular ducts.* That is, there will be higher temperature gradients with the internally cooled plate, and consquently higher stresses.

Since the internally-cooled plate would have both higher temperatures and stresses than the tube design, would probably be slightly harder to fabricate than the tube, and lifetimes in power reactors will probably be limited by neutron irradiation rather than sputtering, I decided to abandon the internally-cooled rectanglar duct design as a practical alternative to the tube.

*Note that the heat flow is two-dimensional, when steady-state is reached. The temperature distribution is not linear. In one dimensional steady-flow in Cartesian coordiantes, the stresses would be zero.

VI. C. STRESS CONCENTRATION FACTORS, FATIGUE AND CREER

VI. C. 1 STRESS - CONCENTRATION FACTORS:

Scratches, notches, grooves, holes, or other abrupt hanges in the cross section of a member may produce higher stresses than the average stresses in the vicinity of such changes. This is called stress concentration. Cracks, slags, incisions, scratches, tool marks, blow holes, and flaws of various kinds produced by manufacturing processes can also contribute to stress concentration.

For example, a hole in a flat plate may produce stresses which are two to three times larger tahn the average stress in the plate a short distance from the hole. It also produces biaxial stresses around the hole; a combined state of stress will change the yeild and ultimate strength of the material. This will make it difficult to predict the strength of members.

Stress values at stress concentration points may be determined by theoretical methods. Experimental testing has shown theory to be accurate. A stress concentration factor defined by

$$Kg = \frac{S_{max}}{S_a}$$

where S_{max} is the maximum stress in the member and S_a is the average nominal stress a short distance from the change in cross section. In fig. 27 are shown measurements of the stress concentration factor for flat plates.

Great care must be taken to avoid areas of high stress in the armour, if notches, grooves, fillets, or holes must be made when mechanically joining the armour to the first wall. Stress concentration should not paly a major role in the calculation of the

maximum stresses in the armour if such changes in cross section are made away from the section of the plate upon which the neutral beam inpinges. For example, if a free plate armour is used, the width of the palte could be slightly larger than the diameter of the neutral beam, and holes could be placed outside the diameter of the beam. Or, if the plate is thick enough, holes could be placed in the plate nearer the section of the plate where stresses are low.

VI. C. 2. Fatigue

Because the neutral beam will be turned on at cyclic intervals, the temperature in the armour of the first wall will undergo cyclic variation, thus causing cyclic thermal stresses. The application of cyclic stress on a material can lead to fracture, even though the applied stress is below the strength of the material. This phenamenon is called fatigue, and depends on the rate of application of the stress, the magnitude and sign (compressive or tensile) of the stress, and the temperatures involved. Fatigue can also be affected by the neutron fluence.

Since the fault condition will occur only rarely if at all, fatigue due to an unattenuated flux wasn't considered. However, the attenuated flux conditon will occur very often, and fatigue due to the normal cycling of the neutral beam should be investiaged.

With fusion power reactors, the stress, during the normal condition, which is built up is negligible for internally-cooled devices or the plates which are cooled on the back-face, and fatigue will not be a concern during this condition. However, for near-term experiment devices which employ radiation-cooled armours, the stress may range

up to several thousand psi for the normal conditon. Fatigue data for graphite or tungsten was not found but Ref. 42 lists fatigue data for Mo at 1153°K which should perform very similarly to N. This data is shown in Fig. 24. The frequency of the tests was generally one HZ. [one MPa = $\frac{1}{6.9 \times 10^{-3}}$ psi]. Since one would expect tungsten's fatigue characteristics to be even better than Molybdenum's, one can estimate that tungsten will not be limited during normal operation by fatigue.

VI. C. 3 CREEP: Creep is the defarmatron with time of a material under a constant stress. Creep may also eventually cause rupture. However, at fusion power conditions, temperature will not be high enough to cause rupture due to creep for either tungsten or graphite. In Fig. 25 is shown the stress vs. time for static creep rupture of molybdenum at 1153°K. One may quickly see that, for tungsten, which would not only have better creep characteristics than No, but also wouldn't reach temperatures of 1153°K, the lifetime will not be limited by creep. The same conclusion can be reached for experimental devices. In Fig. 26 is shown the creep rate vs. temperature for graphite. For anticipated stress levels and temperatures, creep will not be a concern for graphite.

D. SUMMARY

Tungsten on graphite free plates will not fracture or yield under the impingement of an attenuated neutral beam for their respective allowed heat fluxes. Both will probably yield and possibly fracture under the impingement of the allowed unattenuated heat flux. Experimental testing is necessary to determine if fracture will occur and the extent of damage that it incurs. Also, it will be necessary to determine if yielding may be allowed.

Cubes on a backing plate, or small plates on a backing plate, show reduced stresses, but this type of armour will also probably yield under an unattenuated beam strike of an allowed heat flux. ("Allowed heat flux" refers tothe flux allowed with consideration of melting.)

While graphite has a much lower tensile stress than tungsten, the induced thermal stresses are much lower and while tungsten's tensile stress and yield strength decrease with temperature, graphite's strength actually increases with temperature. Graphite is one of only a very few materials which show this characteristic. It will be necessary to experimentally test these two materials to see if yielding or fracture does actually occur, but it seems that graphite would be the more desirable material to use and that for fluxes in the neighborhood of 3-5 MW/cm^2 a graphite plate or cube may be acceptable. Graphite would also be more desirable than tungsten because of graphite's lower atomic number and lower cost.

This backside-cooled, free plate show greatly reduced stresses* and may be applicable to fusion power reactors. However, the stresses that are induced require very good heat transfer between the back face and the coolant tubing, and also were calculated using the assumption that the plate is unrestrained. To achieve the high rate of heat transfer it seems that not only will the plate have to be restrained in some way to maintain contact between the plate and the tubing, but the tubing itself will have to be made of a reasonably strong, high-thermal-conductivity material. (The tubing would have to be fairly strong because high pressures would be required to avoid burnout, and the tubing will be quite thin.) A graphite plate may be set on tungsten tubes; this would allow a low z material to be exposed to the plasma, while still having the highly-conductive, high strength material needed for the tubing.

However, if the plasma impurity confinement time is about the same or less as the plasma particle (D^+, T^+) confinement time, tungsten impurities may not be a very serious problem, and the tungsten tubing could be directly exposed to the plasma. Wall erosion probably would not be the lifetime limiting factor. (See Neutron-Irradiation Section.) Tungsten tubing about 0.3 mm thick would have a structured safety factor of about 1.6 for the refernece power conditions and an unattenuated neutral beam strike. Graphite tubing could not be used because of the high pressure required of the coolant in the event of an unattenuated strike.

*Compared to both the radiation-cooled plate and cube/waffle type of armour.

Because of the higher temperatures and stresses in the rectangular duct, and wall erosion probably wouldn't be the lifetime limiting factor, the rectangular duct design was found not to be competitive with the backside-cooled or tube designs.

Stress concentration will not be a major concern if care is taken about where changes in the cross sections of members are made. Also, because the stresses induced in the armour during normal operation of the fusion reactor will be low, fatigue and creep probably won't be major factors to affect the lifetime of the armour.

VII. SURFACE EFFECTS, WALL EROSION, AND PLASMA IMPURITIES

VII. A. Introduction

Besides adverse thermal conditions, the armour will also be expected to operate under intense ion bombardment and neutron irradiation from the plasma, fusion reaction products, and the neutral beam. These bombarding particles will not only cause damage within the armour, but will also erode the armour and send armour particles into the plasma. These armour particles will deteriorate the performance of the plasma.

One of the main processes which will cause erosion of the armour is called sputtering. Sputtering has been studied for many years and its implications for fusion reactors are a major concern.[23-38] "Physical" sputtering occurs when particles bombard a material with sufficient energy to eject atoms from the surface because of the momentum transfer between the incident particle and the target atom. "Chemical" sputtering occurs when the bombarding particles chemically react with the target atoms to form a volatile compound, which then escapes from the solid. Although both physical and chemical sputtering vary with the energy of the bombarding particle, this effect is more important with the former. Physical sputtering yields (the ratio of the number of atoms ejected to the number of bombarding particles) vary with many parameters. These include the energy of the bombarding particle, the angle of incidence of the bombarding particle, the atomic weights or masses of both the target and the bombarding particle, the target temperature, the surface condition and grain size of the target,

and the dose of bombarding particles.[27]

Although sputtering has been studied for over a century, quantitative agreement between theory and experiment is still hard to achieve, with the a difference factor between theoretical and experimental yields varying up to an order of magnitude. Qualitatively, however, theory and experiment tend to agree. Experimental sputtering yields for D^+, H^+, He^+, and n on a few targets as a function of energy are given in Appendix D. Neutron sputtering have been a subject of controversy till recently. Maminsky found relatively large values for neutron sputtering yields, while Behrisch and others found yields on the order of 10^3 smaller. Maminsky had observed the emission of small chunks of target material, while Behrisch had ovserved only atomic emission. Apparently, as has been recently hypothesized, the chunk emission was due to surface stresses and miscrosstructures in the target material.[32]

A second surface effect that leads to erosion and plasma contamination is radiation blistering. When the gaseous plasma and helium ions escape fromthe plasma and strike the armour, they will slow down due to collisions with the armour atoms. At the end of their respective range, these gaseous particles may collect in small pockets, formed by the displaced armour atoms, and from gas bubbles. As more gaseous particles enter the material the bubbles will grow in size; since the range of these particles is on the order of only a few micros, these growing bubbles may actually deform the surface of the armour, forming visible blisters. Gradually, the pressure within these bubbles becomes so great that it may cause the bubble to burst, not only emitting the enclosed gas, but also ejecting chunks

of armour material into the palsma. Blistering and its fusion reactor implications have also been the subject of intensive study.[27-31,33,34,39] The parameters which govern sputtering yields also affect the extend of blistering damage.

If the temperature of the armour becomes high enough, then some atoms near the surface will have enough energy to be ejected from the material. Evaporation must also be considered as a source of erosion in view of the potentially high temperatures expected for the neutral beam armour. The rate of evaporation depends mostly on the materials's physical properties and on the rate of heat deposition into the material. Behrisch has outlined a simple, clean approach for estimating the amount of material evaporated as a function of the heat depositon rate, or temperature.[30] His results for major first wall candidates are given in Fig. 11.

Other processes which may lead to armour erosion and plasma contamination include photo-desorption of adsorbed or absorbed gases, photo-decompositon of surface compounds, and photo-catalysis. However, not much is known at this point about either the fluxes of photons expected at the first wall, or the extent to which they will effect erosion of materials. Fusion reactor implications are just recently being studied.[52-53]

When impurities get into the plasma, the radiated power is greatly increased because of its dependence on the atomic number Z of the plasma ions. For example, free-free bremsstrahlung radiated power is given by

$$P_B = 0.486 \times 10^{-30} n_e^2 Te^{1/2} \frac{\sum_i Z_i^2 n_i g_{ff} \frac{Z^2}{T}}{\sum_i Z_i n_i} \left[\frac{W}{cm^3}\right]$$

where Z_i = charge on species i in the plasma

Z = charge on the ionized impurity atoms

T = plasma temperature

$g_{ff}(Z^2/T)$ = Gamow Factor

Te = electron temperature

n_e = electron density

and n_i = density of species i in the plasma and recombination radiation is given by

$$P = 1.3 \times 10^{-32} f \frac{Z^4}{T_e^{1/2}} n_e^2$$

where f is the impurity fraction.

As power is radiated away from the plasma, the temperature of the plasma decreases. In addition, at a constant n_e, the impurities cause a decrease in fuel density, which results in a decrease in fusion reaction rates. Thus, as the impurity level is increased, the plasma parameters (density, confinement time, and temperature) required to achieve ignition (when fusion energy equals brensstrahlung losses) and Lawson's Criteria (when electrical output from fusion equls the energy input) became more difficult to achieve. Meade[25] and Behrisch and Kadamtsen[24] have done studies to try to determine the limits on plasma impurities. Their findings are shown in Figs. 12-14. It can easily be seen that : 1) keeping plasma impurities to as low a level as possible is extremely important if

fusion power is to become feasible and 2) materials that are exposed to the plasma should have low atomic numbers if practical.

Unfortunately, classical theory predicts that impurities will tend to migrate toward the center of the plasma; but, only in very quiescent discharges has this been shown to be the case experimentally, and after instabilities have developed the impruities tend to distribute themselves uniformly throughout the plasma. However, one should note that, for several reasons, a small amount of impurities may actually be beneficial to the operation of the reactor: 1) Ohmic heating is made more effective due to the increased resistivity of the plasma, 2) Particle transport is increased, possibly resulting in a more uniform plasma temperature distribution, and 3) Thermal stabilization of the plasma may be necessary at higher temperatures, and this might actually be achieved by radiation losses from the plasma, due to a fractional amount of impurities.[24]

VII. B. Wall Erosion Results

Erosion due to sputtering may be calculated according to the following formulae

$$\Delta\ell = \left(\sum_i S_i \phi_i\right) \frac{3.154 \times 10^8}{n} \eta$$

where $\Delta\ell$ is erosion rate in mm/yr

S_i is the sputtering yield due to species i in atoms/particle

ϕ_i is the flux of species i in particles/cm^2-sec

n is the atomic density of the target in atoms/cm^3

η is the plant efficiency, or up time in %

To calculate the erosion due to blistering a pseudo-blistering yield was used that was calculated assuming that an entire monolayer of material was blistered off after the critical dose for blister rupture had been reached. Thus, the blistering yield is given by [41]

$$S_i = \frac{R_i}{(\phi t)_{c_i}} \frac{N_o \rho}{A_w}$$

where S_i is the blistering yield due to species i, in atoms/particle

R_i is the range of species i into the target material, in cm

N_o is Avagadro's #

ρ is the density of the target material in gm/cm^3

A_w is the atomic weight of the target material

and $(\phi t)_{c_i}$ is the critical fluence for blistering against species i

It was assumed that no blistering occurred after two monolayers had been blistered off. Normally, blistering ceases after a single monolayer has been blasted off, but the above assumption will allow for nonuniformities. An average temperature of $900^{o}K$ was used to calculate erosion rates due to evaporation, using Fig. 11. One fault condition per year was allowed. $900^{o}K$ was used because it is the upper limit for uncooled armours during the normal condition. For cooled "armours", the normal surface temperature will be much lower. Erosion due to photom and electron processes was neglected.

The TFTR anticipated fluxes were used for the near-term device, while for the power reactor flux, those given by Kulcinski[41] for UWMAK were used. These fluxes are given in Appendix D.

The erosion in TFTR was found to be negligible. The tungsten erosion rate, calculated in Appendix D, was found to be 0.018 mm/yr, while the graphite erosion rate was found to be 0.066 mm/yr for the power reactor flux. It would seem that graphite's life may be severely limited by erosion, if it is used as an internally cooled device. For a back-side cooled device or for a radiation cooled armour ∿1 mm - 1 cm thick graphite's life probably would not be limited by erosion due to surface effects. Tungsten remains applicable for any device.

VIII. C. Plasma Impurity Fraction:

The plasma impurity fraction was calculated starting with the following differential equation, equating the rate of change of the impurity fraction to the gain of impurities due to erosion minus the loss of impurities which escape from he plasma.

$$\frac{dN_m}{dt} = (1-\eta)\frac{S_H N_H}{\tau_H} - \frac{N_H}{\tau_m} + (1-\eta)\frac{S_M N_m}{\tau_M} \qquad (26)$$

where N_H, N_M = plasma and impurity concentrations, respectively

S_H, S_M = plasma and impurity erosion yields, respectively

τ_H, τ_M = plasma and impurity confinement times, respectively

η = divertor efficiency

This equation includes the assumption that the eroded armour atoms come off as neutral atoms[30]; otherwise the 1-m term would be squared, because the divertor would eject η% of both the incoming and outgoing ions. Assuming N_H to be constant the solution to the above equation is given by

$$\frac{N_M}{N_H} = \frac{S_H\,(\tau_M/\tau_H)}{\frac{1}{1-m} - S_M}\left(1-e^{S_M(1-m) - 1\,\frac{t}{\tau_M}}\right)$$

We can evaluate an effective overall plasma erosion coefficient by using the following formula

$$S_H = \frac{(\Delta\ell)(n)}{(\phi)(\eta)(3.154 \times 10^8)}$$

where $\Delta\ell$ is now the total erosion and ϕ is the total flux of particles upon the armour. This yields $S_H = 4.21 \times 10^{-3}$ for tungsten and $S_H = 0.027$ for graphite. With $\eta = 0.9$, $\tau_H = 14$ sec, $S_M = 4.0$, and the values of S_H given above, we can graph the impurity fraction for various values of the ratio τ_H/τ_H. This is shown in Fig. 15 and 16. Thus, the tungsten impurity limit is rapidly exceeded if the impurity confinement time is more than about twice as long as the plasma confinement time. Graphite's impurity limit will not be exceeded even for an impurity confinement time that is as much as twenty times the plasma confinement time.

One should remember, however, that other impurities will be present in the plasma, form the first wall, for example and the theoretical plasma impurity limit may have to be lowered. It would appear that, for a tungsten armour, other a short impruity confinement tiem would have to prevail or the divertor efficiency would have to approach 100%. Impurity control for graphite doesn't seem to be a problem.

VIII. NEUTRON IRRADIATION DAMAGE

Even if all of the thermal, stress, erosion, and impurity problems are worked out, the design is still faced with possibly the stiffest test of all: neutron irradiation damage. This is particularly true for fusion power reactors.

Neutron irradiation causes two main effects in materials: 1) displacement of atoms from their equilibrium position in the crystal lattice and 2) transmutation reactions. These two effects lead to a variety of undesirable events such as neutron sputtering; production of gas atoms (primarily hydrogen and helium); production of elements other than those which compose the target material, causing the chemical make-up of the material to be altered; the occurrance of free vacancies and interstitials in the lattice; the production of radioactive species. (Since we have already dealt with neutron sputtering in Section VII.A., I will not discuss it further here.) These effects may in turn cause the formation of voids and gas bubbles, resulting in swelling of the material (fig. 17), swelling due to solid transmutation products, and changes in the physical and mechanical properties of the material. These property changes are usually detrimental to the performance of the material. For example, the thermal conductivity and ductility generally decrease with increasing fluence (figs. 18 and 19); the creep rate is increased and the stress-rupture life is lowered at high temperatures. For materials which display a ductile-to-brittle transition temperature, such as the refractory metals, neutron irradiation causes a shift in this temperature to higher temperatures (fig. 20), i.e.,

the material remains brittle to higher temperatures. However the yield strength of most materials is actually increased due to irradiation (fig. 21). In fact, after a certain amount of irradiation, the yield strength increases to almost the same magnitude as the tensile strength. (The tensile strength doesn't change much with fluence.) This means that the material will remain in the elastic range for larger amounts of stress, and will fracture before much strain is encountered.[43]

Unfortunately, at this time there is no experimental neutron flux available which can simulate the very-high-energy neutron spectrum anticipated for the first wall of fusion power reactors. However, for energies above 0.1 Mev the integral neutron flux in the High Flux Isotope Reactor (HFIR) and in the Experimental Breeder Reactor (EBR-II) can exceed that of fusion power reactors for wall loadings up to 4 MW/M^2. It is expected that "annual atomic displacement rates should be comparable to those achieved in high flux fission reactors and annual gas productio rates should be substantially higher than those achieved in high flux fission reactors." The neutron flux spectrum at the first wall and armor will be the most intense and the hardest in the system.[52]

There isn't much neutron irradiation damage data available for tungsten. One set of data is given in Table XI. However, this set of data shows a decrease in the yield strength and an increase in the relative elongation after irradiation. This may be due to the fact that the test was performed at 200°C, which is probably below the DBTT for tungsten, where tungsten would be brittle to begin with. Other tests with refractory metals show the opposite effects due to radiation

TABLE XI

Effect of Irradiation with Neutrons (5×10^{19} n/cm^2) on the Mechanical Properties of Tingsten Under Tension [12]

Test Temperature, °C		200
Yield Point (kg/mm^2)	Before Irradiation	103.5
	After Irradiation	91.5
Tensile Strength	Before Irradiation	121.1
	After Irradiation	121.1
Relative Elongation	Before Irradiation	2.4
	After Irradiation	4.2

damage (figs. 21 and 22).

There is much more data available on the performance of graphite under neutron irradiation (figs. 18 and 23). The strength of graphite and SiC generally increases, although not to a very great extent, not more than a factor of two. The thermal conductivity is drastically deteriorated due to neutron irradiation. The thermal expansion coefficient is generally decreased by up to a factor of three. The elastic modulus and the modulus of rupture are not significantlt affected.[9]

Ref. 9 lists a possible fluence limit for carbon of 10-20 X 10^{21} neutrons/CM^2, although no basis is given for which this limit is proposed. Using the flux of neutrons in App. D for a fusion power reactor, the life of graphite would be limited to about 1.5 years by neutron irradiation. Neutron cross sections for tungsten in the Mev range are several times those for carbon. Although carbon's atomic density is about twice that of tungsten, the difference doesn't make up for the difference in cross sections. In Table XII are listed the total cross sections for tungsten and carbon at the energies of interest. One may assume that tungsten's fluence limit would certainly be no more than carbon's, implying that tungsten's life would be limited to less than 1.5 years by neutron irradiation damage. Ref. 9 lists SiC's fluence limit between 50 and 100 X 10^{21}, or roughly five times that of graphite.

If conditions can be such that SiC performs adequately thermally and structurally, it would seem to be a better choice of material than either tungsten or graphite. That thermal conditions can be lowered to such an extent remains to be seen.

TABLE XII

σ_{tot} as a Function of Energy For Tungsten and Carbon

Energy (Mev)	Tungsten (barns)	Carbon (barns)
0.001	17.	
0.005	16.	
0.024	13.8	4.78
0.075	13.	4.62
0.120	10.5	4.57
0.62	7.8	3.15
1.0	6.4	2.70
1.5	6.7	2.05
2.0	6.6	1.63
3.0	6.3	1.30
5.0	5.6	1.23
8.0	4.8	1.86
12.0	5.0	1.41
14.0	5.3	1.31

IX. CONCLUSIONS

Near term devices: For near term devices, radiation cooled first wall armors should be adequate, but either the pulse time will have to be shortened or the heat flux lowered from the TFTR neutral beam parameters. It appears that graphite can endure slightly higher heat fluxes than tungsten. Since graphite can't be easily welded to metals, it would have to be either mechanically joined or simply hung on the first wall in some fashion. A graphite plate would be much lighter than a similar tungsten plate. Erosion rates of graphite due to surface effectswill be significantly higher than those for tungsten, but in near-term devices the plasma and neutron fluence isn't expected to be high enough to cause concern, and a graphite armor would be thick enough (on the order of a centimeter thick) to make erosion rates negligible. Besides the graphite would be lower cost and wouldn't cause nearly the same plasma contamination as tungsten. Plasma contamination is an especially important concern if fusion power is to be proved feasible in these near term devices.

Since yielding and possibly fracture will undoubtedly occur for the fault condition for both the plate and the cube designs, and neither will yield for the attenuated condition, it is not considered necessary to employ the cube-type armor, unless it turns out under experimental testing that only yielding will occur with the cube design, while fracture will occur with the plate. At any rate the fault condition should be strictly guarded against. If the heat flux is slightly lowered from the TFTR parameters, yielding may be avoided with graphite, because

graphite's strength actually increases with temperature.

Fusion power reactors: Since power reactors will have much longer neutral beam pulse times (of at least several seconds) and the plasma flux alone will be a significant, constant heat load, ranging up to 1.0 KW/CM^2, fusion reactor first walls will have to be cooled. If fault conditions are allowed, the coolant will undoubtedly have to be at high velocity and high pressure, and the coolant tubing will have to be very thin to handle fault conditions if fault conditions are to be avoided. The high pressure will require a tubing material that has a reasonably high tensile strength (greater than about 25,000 psi at the temperature of concern) as well as good thermal conductivity and mechanical properties. In addition, if the tubing is exposed to the plasma flux it will have to have low sputtering yields since the tubing will be quite thin. The tubing may not have to be directly exposed to the plasma. It may be protected by a thin (less than 2 mm thick) plate, which would be cooled by the tubing. However, it is doubtful that the heat transfer between the plate and the tubing coolant would be high enough to handle the anticipated fault condition and still not crack.

These considerations lead to the following conclusion: if fault conditions would be allowed to occur, then tungsten (or some other high strength, high thermal conductivity, low sputtering material) tubing of about 0.3 mm thickness would have to be employed. The tubing would have to be directly exposed to the plasma. Neutron irradiation damage would probably be the lifetime-limiting factor, rather

than creep, fatigue, or wall erosion. Plasma contamination will be a major concern unless the plasma impurity confinement time is about the same as the plasma confinement time.

If fault conditions could be guaranteed against, a graphite plate could be cooled on the backside by copper tubing for example. (Copper tubing could be used in this case, because the coolant wouldn't have to be highly pressurized, since heat fluxes will be relatively low. Also, the copper tubing wouldn't be exposed to the plasma.) The cost of the tubing system would be drastically decreased, plasma contamination problems from the armor would be practically eliminated, and since neutron irradiation damage would be the lifetime limiting factor, graphite plates 1-2 mm thick would not be seriously damaged by erosion during its lifetime. It seems imperative that some kind of highly efficient safety mechanism be produced to prevent fault conditions from occurring.

REFERENCES

1. J.W.H. Chi and R. Flaherty, "Conceptual Thermal Mechanical Design of the TFTR First Wall Armor Against Neutral Beam Impingement," Proceedings of the Sixth Symposium on the Engineering Problems of Fusion Research, Nov. 18-21, 1975, San Diego, California, IEEE-75CH1097-5-NPS (1975), p. 1180.
2. Alan Y. Lee, "Thermal Analysis of the TFTR Vacuum Vessel Wall Protective Plate," WFPS-TME-015, Oct., 1975, Westinghouse Electric Corporation, Pittsburgh, Pa.
3. R.A. Smith, "Neutral Beam Armor Thermal Stress Analysis," WFPS-TCTR 207, Dec., 1975, Westinghouse Electric Corporation, Pittsburgh, Pa.
4. M.A. Hoffman and R.W. Werner, "Heat Flux Limitations on First Wall Shields for Early Fusion Machines," First Topical Meeting on the Technology of Controlled Nuclear Fusion, April, 1974, San Diego, Ca., CONF-740402-P1 (1974), p. 619.
5. M.A. Hoffman, et. al., "Fusion Reactor First Wall Cooling for Very High Energy Fluxes," Nuclear Engineering and Design, 36, 37 (1976).
6. J.F. Schivell and D.J. Grove, "Thermal Stress Problems in Tokamak Surfaces," Journal of Nuclear Materials, 53, 107 (1974).
7. LBL/LLL CTR Staff, "TFTR Neutral Beam Injection System Conceptual Design," Lawrence Berkeley Lab Report LBL-3296 (1975).
8. J. Kim, et. al., "Design Considerations of Calorimeter Target for High Power Neutral Beam Injectors," Proceedings of the Sixth Symposium on Engineering Problems of Fusion Research, Nov. 18-21, 1975, San Diego, Ca., IEEE-75CH1097-5-NPS (1975).
9. L.H. Rovner and G.R. Hopkins, "Ceramic Materials for Fusion," Nuc-

lear Technology, 29, 274 (1976).

10. H.S. Carslaw and J.C. Jaeger, Conduction of Heat in Solids, Second Edition, Oxford University Press (1959).
11. B.A. Boley and J.H. Weiner, Theory of Thermal Stresses, John Wiley and Sons, Inc. (1960).
12. M.A. Filyand and E.I. Semenova, Handbook of the Rare Elements, Vol. III, Boston Technical Publishers, (1970).
13. Refractory Ceramics for Aerospace, A Materials Selection Handbook, Batelle Memorial Institute, Columbus, Ohio, American Ceramic Society Inc. (1964).
14. C.J. Smithells, Metals Reference Book, Fifth Edition, Butterworths, London (1976).
15. M. Jakob, Heat Transfer, Vol. I, John Wiley, New York (1958).
16. A. Edwards, "TRUMP, A Computer Program for Transient and Steady State Temperature Distributions in Multidimensional Systems," Lawrence Livermore Lab Report UCRL-14754, Rev 3 (1972).
17. F. Kreith, Principles of Heat Transfer, Third Edition, Intext Press Inc. (1973).
18. M.M. El Wakil, Nuclear Heat Transport, International Textbook Co. (1971).
19. K. Wark, Thermodynamics, Second Edition, McGraw Hill Book Co. (1966).
20. K.J. Bathe, E.L. Wilson, and F.E. Peterson, SAP IV, A Structural Analysis Program for Static and Dynamic Response of Linear Systems, Earthquake Engineering Research Center Report EERC-73-11, University of California, Berkeley (1974).
21. S. Timoshenko and J.N. Goodier, Theory of Elasticity, Second Edition, McGraw Hill Book Co. (1951).

22. W.R. Gambill, R.D. Bundy, and R.W. Wansbrough, "Heat Transfer, Burnout, and Pressure Drop for Water in Swirl Flow through Tubes with Internal Twisted Tapes," Oak Ridge National Lab Report) ORNL-2911 (1960).

23. R. Behrisch and W. Heiland, "Influence of Wall Material on Plasma-Wall Interaction," Proceedings of the Sixth Symposium on Fusion Technology, Sept. 22-25, 1970, Aachen, Germany, EUR-4593-e (1970), p. 461.

24. R. Behrisch and B.B. Kadomtsev, "Plasma Impurities and Their Significance in Fusion Reactors," Fifth Conference Proceedings on Plasma Physics and Controlled Nuclear Fusion Research, Vol. II, Nov. 11-15, 1974, Tokyo,IAEA-CN-33/S 2 (1974), p. 289.

25. D.M. Meade, "Effect of High-Z Impurities on the Ignition and Lawson Conditions for a Thermonuclear Reactor," Nuclear Fusion, 14, 289 (1974).

26. H.A.B. Bodin and G.M. McCracken, "Startup and Associated Wall Problems in Toroidal Fusion Reactors," Fifth Conference Proceedings of Plasma Physics and Controlled Nuclear Fusion Research, Vol. II, Nov. 11-15, 1974, Tokyo, IAEA-CN-33/S 4 (1974), p. 303.

27. M. Kaminsky, "Plasma Contamination and Wall Erosion in Thermonuclear Reactors," IEEE Transactions in Nuclear Science, 18, 208 (1971).

28. T.D. Ros, S.K. Das, and M. Kaminsky, "Reduction of Surface Erosion in Fusion Reactors," Journal of Vacuum Science Technology, 14, #1, 550 (1977).

29. M. Kaminsky and S.K. Das, "Surface Erosion Phenomena in Connection with CTR Aplications," To appear in the Proceedings of the Fourth Conference on the Use of Small Accelerators, October 25-27, 1976,

Denton, Texas.

30. R. Behrisch, "First Wall Erosion in Fusion Reactors," Nuclear Fusion, 12, 695 (1972).

31. M. Kaminsky, "Plasma Contamination and Wall Erosion in Controlled Thermonuclear Fusion Devices and Reactors," Fifth Conference Proceedings on Plasma Physics and Controlled Nuclear Fusion Research, Vol. II, Nov. 11-15, 1974, Tokyo, IAEA-CN-33/S3-3 (1974), p.287.

32. P. Dusza, S.K. Das, and M. Kaminsky, "Neutron Sputtering of Solids," Advances in Chemistry Series #158, Radiation Effects on Solid Surfaces (1976).

33. G. Carter and J. Colligan, Ion Bombardment of Solids, American Elsevier, New York (1968).

34. M. Kaminsky, Atomic and Ionic Impact Phenomena on Metal Surfaces, Springer- Verlag, New York (1965).

35. A.J. Summers, N.J. Freeman, and N.R. Daly, "Sputtering Coefficients of Niobium," BNES Nuclear Fusion Reactor Conference, Culham Lab, Sept. 1969, p. 347.

36. G. Haas, "On the Interaction of Sputtered Wall Material with Fusion Plasma," Proceedings of the Sixth Symposium on Fusion Technology, Sept. 22-25, 1970, Aachen, Germany, EUR-4593-e (1970), p. 471.

37. A.J. Summers, N.J. Freeman, and N.R. Daly, "Sputtering of Niobium by Niobium, Hydrogen, and Helium Ions in the 10- to 80- Kev Range," Journal of Applied Physics, 42, #12, 4774 (1971).

38. G. Rosenburg and G.K. Weiner, "Sputtering Yields for Low Energy He^+-, Kr^+-, and Xe^+-Ion Bombardment," Journal of Applied Physics, 33, #5, 1843 (1962).

39. S.K. Das and M. Kaminsky, "Radiation Blistering in Metals and Al-

loys," Advances in Chemistry Series #158, Radiation Effects on Solid Surfaces, (1976).

40. TCT, Two Component Torus, Joint Conceptual Design Study, Vol. III, Plasma Physics Lab, Princeton, New Jersey and Westinghouse Electric Corporation, Pittsburgh, Pa. (1974), p. 6-105.

41. G.L. Kulcinski and G.A. Emmert, "First Wall Surface Problems for a D-T Tokamak Reactor," Journal of Nuclear Materials, 53, 31 (1974).

42. R.A. Yeske, W.V. Green, and E.G. Zukas, "The Tensile Fatigue Behavior of Molybdenum at 1153^{o}K," Proceedings of the First Topical Meeting on the Technology of Controlled Nuclear Fusion, April 16-18, 1974, San Diego, Ca., CONF-740402-P2 (1974), p.456.

43. G.L. Kulcinski, "Radiation Damage by Neutrons to Materials in D-T Fusion Reactors," Fifth Conference Proceedings on Plasma Physics and Controlled Nuclear Fusion Research, Vol. II, Nov. 11-15,1974, Tokyo, IAEA-CN-33/S 3-1 (1974), p. 251.

44. G.L. Kulcinski, "Radiation Damage: The Second Most Serious Obstacle to the Commercialization of Fusion Power," CONF-750989.

45. F.W. Wiffen, "The Effects of CTR Irradiation on the Mechanical Properties of Structural Materials," Oak Ridge National Lab Report ORNL-TM-5624 (1976).

46. E.E. Bloom, F.W. Wiffen, and P.J. Maziasz, "Temperature and Fluence Limitations for a Type 316 Stainless Steel CTR First Wall," Oak Ridge National Lab Report ORNL-5082 (1976), p. 18.

47. B. Badger, et.al., "A Wisconsin Toroidal Fusion Reactor Design," University of Wisconsin Report UWFDM-68 (1974).

48. B. Badger, et. al., "A Conceptual Tokamak Reactor Design, UWMAK-II," University of Wisconsin Report UWFDM-112 (1975).

49. B. Badger, et. al., "A Non-Circular Tokamak Power Reactor Design," University of Wisconsin Report UWFDM-150 (1976).

50. W.M. Stacey, D.L. Smith, and J.W. Brooks, "Impurity Control in Near Term Tokamak Reactors," Proceedings of the Second Topical Meeting on the Technology of Controlled Nuclear Fusion, Vol. I, Sept. 21-23, 1976, Richland, Washington, CONF-760935 (1976), p. 315.

51. G.F. Barnett, et. al., "Atomic Data for Controlled Nuclear Fusion Research," Oak Ridge National Lab Report ORNL-5207 (1977).

52. D. Steiner, "The Technological Requirements for Power by Fusion," Nuclear Science and Engineering, 58, 107 (1975).

53. R.J. Hoverton, "Tabulated Neutron Cross Sections 0.001- 14.5 Mev," Lawrence Radiation Lab Report UCRL-5226 (1959).

54. Conversation with Dr. R.V. Pyle, Lawrence Berkeley Lab.

APPENDIX A

DISCUSSION OF COMPUTER CODES

(TRUMP AND SAP4)

1. TRUMP:

TRUMP was used to calculate temperature distributions in the various designs, both as a check on analytical solutions and as a solution for designs for which analytical solutions would be either very complex or would be practically impossible to obtain due to unusual geometries, boundary conditions, etc. It solves "a general nonlinear parabolic partial differential equation describing flow in various kinds of potential fields, such as fields of temperature, pressure, and electricity and magnetism; simultaneously it will solve two additional equations representing, in thermal problems, heat production by decomposition of two reactants having rate constants with a general Arrhenius temperature dependence." TRUMP allows for three-dimensional geometry, involving simple or complex structures, a wide variety of iniital and boundary conditions, and can work in either Cartesian, cylindrical, or spherical coordinates. It can find solutions for either transient or steady-state problems. The average amount of computer time ranges from 0.3 to 2 msec per time step for each modal paint and connection between modal paints. Although written primarily in Fortran IV, it is readily adaptable to most computer systems.[16]

SAP4 (Structural Analysis Program):

Once the temperature distributions were found by TRUMP, they were imput into SAP4, which computed the thermal stress distribution. SAP4 is a finite element program for application to static and dynamic analysis of linear structural systems. I used SAP4 with a static analysis. In this mode, SAP4 solves the equations of equilibrium followed by the computation of the element stresses. The program's capacity is mainly dependent ypon the computer used, the number of modal paints used to describe the structure, and the number of eigenvalues if dynamic analysis is required. Up to six displacement degrees of freedom are allowed for each mode and there is practically no limit on the number of elements, the number of load cases, or the order and bandwidth of the stiffness matrix. The program can work with one-, two-, or three-dimensional systems. It is written in FORTRAN IV and operates without modification on the CDC 6400, 6600, and 7600 computers. A program for non-linear analysis NONSAP is also now available.

Linear vs. Nonlinear, Elastic vs. Inelastic, and Static vs. Dynamic

Most materials generally conform to the main requirements of linear, elastic thermal stress analysis at low temperatures and low stress levels. These requirements include a) small strains, b) strains related to the stresses by a linear equation (the material behaves elastically at all times) and c) the temperature may be determined independently of the deformations of the body. The first assumption implies that the displacements are small enough that no distinction need be made between the coordinates of a particle before and after

deformation, and that the displacement gradients are small enough that their products are negligible. Finally, the third assumption requires the omission of mechanical coupling terms in the heat conduction equation.

For the unattenuated heat flux upon uncooled armours, the temperatures are too large for this kind of analysis, but SAP4 should still give good qualitative results. Since yielding will occur, empirical stress-strain curves will be required to determine if fracture will occur; better yet, experimental analysis should be performed. The attenuated heat flux will not cause large stresses or strains so the linear, eleastic analysis will be adequate This should also be the case for the unattenuated heat flux upon internally-cooled devices.

Static analysis, as opposed to dynamic analysis, should apply if the pulse time to and thermal diffusion time τ_T are much greater than the characteristic mechanical time τ_M. For plates τ_T is given by $\frac{L^2}{K}$ and for tubes by $\frac{c_\rho \rho(n_o^2 - n_o^2)}{4K}$. τ_o is at least 500 msec. We may find τ_M by the formulas

$$B = \frac{t_T}{t_M} = \frac{L}{a\sqrt{K}} \left(\frac{D}{L_q}\right)^{1/4} \quad \text{and} \quad D = \frac{EL^3}{12(1 - \nu^2)}$$

where a is the length of a side of a square plate and other parameters have been defined in the text. Thus, for a 1 cm thick plate, 0.5 m x 0.5 m, we find t_M - 0.0181 sec for tungsten and t_M = 0.0362 sec for graphite. Since t_T = 1.88 sec and 0.862 sec respectively, a static analysis would seem to be adequate.

APPENDIX B

COOLANTS, HEAT TRANSFER COEFFICIENT, AND BURNOUT HEAR FLUX

COOLANTS:

If coolants are used to help the thermal and mechanical performance of the armour, amny additional considerations must be made. If coolant must be chosen on the basis of its thermal performance, its cost, corrosive properties, and its performance in the vicinity of high electromagnetic fields ans neutron bombardment. There are gases, inorganic liquids, molten metals, and organics to choose from. A structural safety factor (ratio of the yield stress to the total stress in the material) must be employed. The probability of leaks is greatly increased with the introduction of inelastic deformation, so the safety factor must be greater than unity. The cost of the design is going to be significantly increased due not only to the the increased complexities of the design, but also because work will be required to pump the coolant, and the cost of the coolant itself may be significant. The replacement and repair of the device will be more difficult. The thickness of the material between the surface and the coolant will have to be thin enough to take advantage of th e coolant, but thick enough that it's lifetime isn't significantly reduced due to the erosive actives of surface effects. This may be the most difficult of all of the coolant considerations to cape with care must be taken not to exceed the burn-out heat flux. Finally it should be noted that the "armour" may need to be the first wall itself if internal coolants are employed.

I didn't spend too much time choosing a coolant. Water is not only highly available and has essentially no cost, but has a relatively good heat transfer coefficient, requires relatively little pumping work in relation to the heat it removes, and water has been throughly documented. It isn't terribly corrosive. The following table lists heat transfer coefficients, for various categories of coolants, and the ratio of required pumping work to the amount of heat removed normalized to 1.0 for water. Organics have been known to break down

TABLE B1

Coolant Performance in Fission Power Reactors

Coolant	h Btu/hr $ft^2{}^oF$	W/q(relative)
Light and heavy water	5000-8000	1.0
Organic liquids (polyphenyls, etc.)	2000-3000	4-10
Liquid metals (sodium, sodium-potassium alloys, etc.)	4000-10,000	3-7
Gases (He, CO_2, N_2, air, etc.)	10-100	~100

at relatively high temperatures, liquid metals are particularly corrosive, and gases have poor thermal performance.

Heat Transfer Coefficient:

The heat transfer coefficient can be calculated from one of several correlations. For large temperature drops across the surface film layer, the best-known correlation is probably the Sieder-Tate equation for flow in circular tubes:

$$Nu = 0.023\ Ro^{0.8}\ Pr^{0.4}\ \left(\frac{M_w}{\mu_o}\right)^{0.14}$$

where Nu is the Nusselt number, Re is the Reynold's number, Pr is the

Proudth number, and μ_w and μ_o are the viscosities of the water at the wall temperature and bulk temperature respectively. N_u, R_e, and Pr are defined by $Re = \frac{\rho V D_e}{\mu_o}$, $Nu = \frac{hD_e}{K}$, and $Pr = \frac{C_p \mu_o}{K}$, where V is the coolant velocity, ρ is the coolant density, C_p is the specific heat, K is the thermal conductivity, De is the equivalent diameter of the coolant passage, and h is the heat transfer coefficient. For flow in non-circular ducts, De is given by $De = 4Ac/p$ where Ac is the cross sectional area of the flow channel and P is the wetted perimeter of the hammel.[18]

A correlation has been developed for tubes with internal twisted tapes to enhance heat transfer.[22] It is given by

$$h = \frac{2.18}{y^{0.09}} \quad \frac{0.023}{(pr)^{2/3}} \quad \frac{1 + (D_e/L_H)^{0.7}}{Re^{0.2}} \quad C_p G$$

where G is ρV, the mass flow rate per unit area, y is the tape-twisted ratio defined by 180^o twist axial length divided by De. Presumably, if large temperature drops occur across the wall surface film layer, one should multiply this correlation by the Sieder-Tate fraction $\left(\frac{\mu_w}{\mu_b}\right)^{0.14}$.

The heat transfer coefficient is given as a function of coolant temperature in the table below with y = 2.5, De = 10mm, L - 1.0 m, and pressure of the coolant set at 2000 psia. I've also assumed a wall temperature of 800^oK

TABLE

HEAT-TRANSFER COEFFICIENT VS. COOLANT VELOCITY AND TEMPERATURE

$T\ ^{o}R$	$h_{T.T}$	$h_{S.T.}$	$h_{T.T.}$	$h_{S.T.}$	$h_{T.T.}$	$h_{S.T.}$
683 293	64,900	37,400	113,000	65,100	156,000	90,000
400.835	223,500	110,000	389,000	191,000	538,000	264,000
488.905		138,000		240,000		332,000
600.949		138,000		241,000		332,000

$h_{T.T}$ = twisted tape heat transfer coefficient assuming that the Sieder-Tate factor is used $[u/K^2 - {}^{o}K]$

$h_{S.T.}$ = Sieder-Tate heat transfer coefficient $[w/\mu^2 - {}^{o}K]$

I chose a pressure of 2000 psi because water has a high saturation temperature at high pressures, which would essentially allow me to much less cautious about burnout, and the viscosity, (and consequently μ_w) is higher at higher pressures, which increases the heat transfer coefficient.

While swirl tubes drastically increase the heat transfer coefficient, they would add to the cost of the system. It is doubtful that they will be required for the reference heat flux but if future beam heat fluxes are more than 10 $\mu w/cm^2$, then swirl tubes might be employed.

Thus, for calculations and input for TRUMP I used the following heat transfer coefficients: at V = 70 μ/sec, $h = 73{,}500 \frac{w}{m^2 - {}^{o}K}$; at V = 60 m/sec, $h = 1.28 \times 10^5 \frac{w}{m^2 - {}^{o}K}$; and at V = 90 m.sec, $h = 1.77 \times 10^5 \frac{w}{m^2 - {}^{o}K}$

PRESSURE DROP

The pressure drop $\Delta\rho$ may be calculated using the Darsy formula:

$$\Delta\rho = f \frac{L_H}{De} \frac{\rho V^2}{2qc}$$

where f is the friction factor and qc is a conversion factor, $qc = 4.17 \times 10^8 \frac{lb_m - ft}{lb_f - hr^2}$. The friction factor depends not only on the Reynold's number of the coolant, but also on the roughness of the tubing material f may be found from either the Moody friction factor chart, or, for smooth tubing, f is given approximately by

$$f = \frac{0.184}{Re^{0.2}} \left(\frac{\mu_o}{\mu_w}\right)^{0.25}$$

Since f and ρ and consequently $\Delta\rho$ are functions of temperature, ideally the pressure drop should be evaluated at small intervals along the length of the tubing ans summed together. I used the average temperature of the coolant along the tubing length to evaluate f, ρ, and $\Delta\rho$. I also assumed that the roughness of the tubing corresponded to that of drawn tubing.

Pumping Work:

The pumping work required due to pressure losses is given by

$$W = \Delta\rho AcV = f \frac{L_H}{De} \rho \frac{V^3}{2qc} Ac$$

Increasing the velocity may aid the heat transfer coefficient, but it increases the pressure drop ans pumping work to an even greater degree.

Burn-Out

The burn-out heat flux and its measurement have been the subject of much study. Burn-out, or boiling crisis, occurs when the heat flux through the tubing walls (or the temperature difference between the channel wall and the bulk coolant) exceeds a "certain" value; the temperature of the tubing wall may suddenly, drastically increase, possibly causing rupture of the tubing, due to either melting or thermal stresses or both. This certain value is called the "burn-out heat flux", and occurs at the departure from boiling, ΔNB. If δ, the mass fow rate, is too small, the channel wall temperature may become too high. If δ is too large the pressure drop may be exceedingly large, causing a drastic lowering of the bulk saturation temperature.

One must be careful about the magnitude of the mass flow rate.

There are several correlations available to calculate the critical heat flux for subcolled flow. One, called the ANL Correlation is given by

$$qc'' = C \left(\frac{G}{10^6}\right)^M (t_{sat} - t_{bulk})^{0.22}$$

where t_{sat}, t_{bulk} are the saturation and bulk temperatures in ^oF respectively at the point of burnot and c and m are constants depending on the pressure of the coolant. The mass velocity range covered by the above correlation is 0.96×10^6 to 7.8×10^6 lbn/ft^2 - hv, and the range of subcooling is 5.5 to 163 ^oF.

Another correlation, the Raussar correlation, is given by

$$qc'' = D_1 + D_2V(t_{sat} - t_{bulk})$$

where D_1 and D_2 are constants: $D_1 = 8.34 \times 10^6 \ \frac{w}{m^2}$ and $D_2 = 8.31 \times 10^3 \ \frac{J}{m^3 - {}^oC}$. According to Raussor, this equation is valid for subcooled flow in the range $V(t_{sat} - t_{bulk}) \geq 850^oC$ m/sec, i.e. for high velocity and high subcooling conditions.[5] Other correlations may be found in Ref. 18 and 22, but the Raussor correlation seems adequate for our purposes.

As an example let us calculate a hypothetical pressure drop, pumping work, and burn-out flux, using V = 60 m/sec p = 2000 psi, an average bulk coolant temperature of 375^oK, L = 1.0 m, D_e = 10 mm. First, the pressure drop must be calculated and the corresponding T_{sat} at the end of the tube must be found. I found the Reynold's number to be 2.02×10^6, which for drawn tubing gives f = 0.0135. Using the Darcy formula for the pressure drop, I found $\Delta\rho$ = 339 psi, which temperature is 375^oK. Since the average bulk temperature is 375^oK, the exit bulk temperature would be, assuming an inlet temperature of 300^oK, 450^oK. Thus, the burn-out heat flux would be, using the Raussor correlation,

$$qc'' = 8.34 \times 10^6 + (8.31 \times 10^3)(60)(594 - 450)$$

$$= 8.01 \ KW.cm^2$$

The reference heat flux would not exceed the burnout heat flux. The pumping work required would be

$$W = \Delta\rho \frac{\pi D^2}{4} V = (315)\pi \frac{(0.03281)^2}{4} \ (196.9)$$

$$= 7551 \ \frac{ft - lb}{sec}$$

$$= 10.2 \ KW$$

One must remember though that heat is being removed at a rate of about 7 KW/cm^2 so less than 10 kW would be actually required by outside systems.

APPENDIX C

PHYSICAL PROPERTIES

	W		Graphite		Mo		SiC	
T °K	K	Cp	K	Cp	K	Cp	K	Cp
293.0	164.8	134.9	180.0	72.1	132.1	256.6	173.0	680.0
400.0	156.6	138.1	173.8	994	126.7	261.1	152.9	783.
600.0	136.9	138.1	121.4	1405	118.0	273.9	116.4	927.
800	119.8	138.4	73.5	1656	111.8	286.3	80.0	1040.
1000	110.4	148.3	62.8	1792	109.0	292.3	56.0	1117.
1500	99.9	155.6	50.2	2008	105.3	327.2	21.4	1340
2000	96.1	159.0	50.2	2109	104.7	338.9	15.0	1566.
2500	94.0	159.0	50.2	2183	104.7	338.9	15.0	1677.
3500	93.5	159.0	50.2	2238	104.7	338.9	15.0	~1740.
4000	93.5	159.0	50.2	2601				
ρ	19,295.0		2159.		10,213.		3100.	
T_{melt}	3643		3873		2883		2973	

$$[\mu] = \frac{W}{m - {}^{o}K}$$

$$[Cp] = [J/Kg]$$

MECHANICAL PROPERTIES

	W					Graphite				
	α	E	σ_{tens}	σ_{comp}	$\sigma_y[10^7 \frac{N}{m^2}]$	α	E	σ_{tens}	σ_{comp}	σ_y
293	4.7	40.7	193	152		2.6	1.17	2.0	3.38	
500	4.8	40.0		139		3.0	1.18	2.03	3.45	
1000	5.1	38.7		68		3.9	1.20	2.14	3.76	
1500	5.8	36.0		30		4.3	1.27	2.41	4.14	
2000	6.8	31.9		8		4.8	1.59	2.74	4.65	
2500	8.0	26.2		2.0		5.0	1.65	3.38	5.52	
3000	9.8	15.5		1.0		5.4	1.59			
3500	11.0	7.4		1.0		5.5	1.45			
4000	12.2	6.0		1.0		5.7				
ν	0.28					0.23				

$[\alpha] = [10^{-6}/K^{o}]$

$[E] = [10^{10} N/m^2]$

$[\sigma] = [10^{7}\ N/m^2]$

APPENDIX D (Part I)

SPUTTERING YIELDS VS. ENERGY

	0.5	1.0	3.0	5.0	10.0	20.0	30.0	50.0	100.0	200.0	500.0	3500
Tungsten		0.00072	0.00095	0.00093	0.00089	0.00079	0.00070					
Graphite			0.03		0.05	0.05	0.04	0.02	0.01			
Moly		0.0029	0.0037		0.0062	0.01		0.0079	0.0046	0.0026	0.0012	
SiC			0.015		0.015							
					HT							
Tungsten		0.00023	0.00029	0.00032	0.00038							
Graphite			0.024	0.018	0.009		0.006	0.003	0.002			
Moly		0.0017	0.0024	0.0028	0.0036							
SiC				0.009	0.006							
					He^{++}							
Tungsten	0.0069	0.01										
Graphite	0.067	0.11	0.13	0.12	0.095	0.073	0.07	0.06	0.05			
Moly	0.031	0.051										
SiC		0.15	0.15	0.15								

14.1 MeV Neutrons

APPENDIX D (Part I Cont'd)

	0.5	1.0	3.0	5.0	10.0	20.0	30.0	50.0	100.0	200.0	500.0	3500
Tungsten	$\leq$0.011											
Graphite	$\sim 10^{-4}$											
Moly												
Sil	$\sim 10^{-4}$											
				Self-Sputtering								
Tungsten	0.9	1.61	$\sim$2.9	$\sim$3.4	$\sim$4.0	$\sim$4.5	$\sim$4.6	$\sim$4.9				
Graphite	0.35	0.36	0.37	0.38	0.39	0.40	0.41	0.40				
Moly							$\sim$2.0	$\sim$2.2				
Sil	0.54	0.64										

APPENDIX D (Part II)

WALL EROSION AND PLASMA IMPURITY CALCULATIONS

TUNGSTEN:

SPUTTERING: First, we must know the fluxes anticipated at the armour. Kulciuski gives fluxes for UWMAK as

SPECIES	FLUX [cm^{-2} - sec^{-1}]	ENERGY [KeV]
D^+	6.4×10^{13}	23
T^+	6.4×10^{13}	23
He^+	4.7×10^{12}	23
He^+	1.7×10^{11}	100
n	9.4×10^{13}	>10,000
n	3.4×10^{14}	100 - 10,000
Fe^+	2.5×10^{12}	23

Important plasma parameters includes:

PLASMA DENSITY	$8 \times 10^{13}/cm^3$
PLASMA TEMPERATURE	11 keV
CONFINEMENT TIME	14 sec
MAJOR RADIUS	13 m
MINOR RADIUS	5 m
FIRST WALL MATERIAL	
DIVERTOR - POLOIDAL, DOUBLE NULL: 90% EFFICIENT	
POWER	5000 MW
FRACTIONAL BURNUP	7.2%

In Ref. 40, TFTR fluxes and parameters are given as

SPECIES	FLUX [cm^{-2} - sec^{-1}]	ENERGY (keV)
D^+	8×10^{15}	3
T^+	8×10^{15}	3
n	5×10^{12}	14,100
n	2×10^{13}	thermal - 14,100
α	5×10^{12}	3,500

PLASMA DENSITY	5×10^{13} cm^{-3}
PLASMA TEMPERATURE	5.0 keV
MAJOR RADIUS	2.5 m
MINOR RADIUS	0.85 m
CONFINEMENT TIME	~0.2 sec
FIRST-WALL MATERIAL	Stainless steel
DIVERTOR	None
POWER	1 w/cm^3
FRACTIONAL BURNUP	

Plasma Flux:

Now we simply multiply the flux by the sputtering yield at the energy of interest, assuming uniform fluxes upon the armour.

D^+	$(6.4 \times 10^{13})(7.7 \times 10^{-4})$	$= 4.93 \times 10^{10}$
T^+	$(6.4 \times 10^{13})(7.7 \times 10^{-4})(1.5)$	$= 7.40 \times 10^{10}$
He^+	$(4.7 \times 10^{12})(\sim 0.007)$	$= 3.29 \times 10^{10}$
He^+	$(1.7 \times 10^{11})(\sim 0.0007)$	$= 1.19 \times 10^{8}$
n	$(9.4 \times 10^{13})(\sim 10^{-3})$	$= 9.4 \times 10^{10}$
n	$(3.4 \times 10^{14})(\sim 10^{-4})$	$= 3.4 \times 10^{10}$
Fe	$(2.5 \times 10^{12})(\sim 1.5)$	$= 3.75 \times 10^{12}$

$$4.03 \times 10^{12} \ \frac{\text{atoms}}{\text{cm}^2 - \text{sec}} =$$

20.2×10^{-3} mm/yr

Neutral Beam:

For a 10 Kw/cm^2 neutral beam, the flux fo particles is about 6.25×10^{17} cm^{-2} sec^{-1}, assuming that the average energy of the beam particle is about 100 keV. If the beam undergoes 98% attenuation by the plasma, then its magnitude at the armour would be 1.25×10^{16} cm^{-2} - sec^{-1}. At 100 keV the extrapolated sputtering yield for W si about 4.5×10^{-4} for deuterium. Remembering that the incident beam particles will be at least at our angle of 45^o to the surface of the armour we find that

$$\Delta\ell_{beam} = \frac{(1.25 \times 10^{16})(4.5 \times 10^{-4})}{\cos 45} = 7.96 \times 10^{12} \text{ atoms/cm}^2 - \text{sec}$$

The neutral beam pulse times for future machines in not known at this time, but estimates begin at several seconds. Assuming a beam time of 20 seconds and a cycle time of 500 seconds, the erosion rate by the neutral beam would be roughly 1.59×10^{-3} mm/yr.

Blistering: Assuming that the range of helium ions in tungsten is about 1 microm and that the critical fluence for blistering is about $10^{19}/cm^2$, we find a pseudo blistering yield for He ions on W of 0.63. Hydrogen blistering is not expected to occur to a significant degree in W. Thus the erosion due to blistering is

$$(4.9 \times 10^{12})(0.63) = 3.09 \times 10^{12} \text{ atoms/cm}^2 - \text{sec}$$

Assuming only two monolayers are blistered off and recognizing that the time for the critical fluence to accumulare is $\sim 2 \times 10^6$ sec, we find the total erosion in the first year of operation due to be 1.96×10^{-3} mm.

Evaporation: Using Fig. XII, the evaporation rate of tungsten at $900^{\circ}K$ is completely negligible. Even for a fault condition, allowing the temperature to approach the melting point, erosion due to evaporation is not significant.

Self-sputtering: Assuming that the tungsten impurity flux will be at least a factor of 10^2 smaller than the Fe impurity flux because of its (W's) much lower erosion rate and W will only cover a small fraction of the first wall area, the tungsten flux at the armour should be no greater than 2.5×10^{10}. This yields a self-sputtering erosion rate of

$$(2.5 \times 10^{10})(4.5) = 1.13 \times 10^{11} \text{ atoms/cm}^2\text{-sec} = 5.6 \times 10^{-4} \text{ mm/yr}$$

Totals: For the first year of operation we would have a total erosion of 1.94×10^{-2} mm and for successive years, 1.79×10^{-2} mm/yr, assuming that the reactor is "up" 80% of the year.

Graphite: Going through the same process for graphite we arrive at an erosion rate of 0.0671 mm in the first year and 0.0655 mm/yr in successive years. Chemical sputtering accounted for about 15% of the total erosion for graphite. I briefly recount my calculations below:

SPUTTERING	D^+	$(6.4 \times 10^{13})(0.05)$	$= 3.2 \times 10^{12}$
	T^+	$(6.4 \times 10^{15})(0.05(1.5)$	$= 4.8 \times 10^{12}$
	He^+	$(4.7 \times 10^{12})(0.072)$	$= 3.38 \times 10^{11}$
	He^+	$(1.7 \times 10^{11})(0.0072)$	$= 1.22 \times 10^{9}$
	n	$(9.4 \times 10^{13})(10^{-4})$	$= 9.4 \times 10^{9}$
	n	$(3.4 \times 10^{14})(0.002)$	$= 6.8 \times 10^{11}$
	Fe	$(2.5 \times 10^{12})(2.0)$	$= 5.0 \times 10^{12}$
	C	$(2.5 \times 10^{11})(0.4$	$= 1.0 \times 10^{11}$
			$14.1 \times 10^{12} \frac{\text{atoms}}{\text{cm}^2\text{-sec}} = 0.0394 \frac{\text{mm}}{\text{yr}}$

Blistering:

$$S = \frac{R}{(Qt)c} \frac{N_o \rho}{Aw} = \frac{(10^{-4})(6.02 \times 10^{23})(2.25)}{(10^{19})(12)} = 1.13 \frac{\text{atoms}}{\text{particle}}$$

$$\Delta \ell_{DL} = (1.13)(4.9 \times 10^{12} \frac{\alpha}{\text{cm}^2 - \text{sec}} (2) = 10.1 \times 10^{12} \text{ atoms/cm}^2\text{-sec}$$

$$= 1.96 \times 10^{-3} \text{ mm in the first year}$$

I neglected hydrogen blistering, because a blistering was shown to be negligible also.

Evaporation: Evaporation was again shown to be negligible

Beam Sputtering: $(1.25 \times 10^{16})(0.01) = 1.25 \times 10^{14}$ atoms/cm^2 - sec

= 0.0353 mm/yr with a 20 sec pulse time and a 500 sec cycle time.

Chemical Sputtering: The peak in the chemical sputtering yield curve occurs at about 600°C.[47,49] Since for steady state operation the graphite would have to be cooled, the normal temperature would be below this. For experimental reactors the average uncooled graphite temperature should be at least 150°C above this, at about 750°C. For 23 keV, D^+ and T^+ an a graphite target about 500°C or 700°C is about 0.03. At 400°C, the yeild drops to about 5×10^{-3}, and for lower temperatures levels off at about 4×10^{-3}. Conservatively, I chose a chemical sputtering yield of about 0.02, which, when multiplied by the sum of the D^+ and T^+ fluxes, yields an erosion rate of 7.14×10^{-3} mm/yr. Remember that for certain designs these erosion totals must be increased even further because of angle considerations. For example, for the tube design, we would have to increase the sputtering erosion totals by at least a factor of two.

Note that while the TFTR has a much high anticipated flux than the power reactor, it isn't expected to be up anywhere near 80% of the time. Indeed, Ref. 40 estimates the maximum erosion of the first wall to be less than 10^{-4} mm for the total life of the experiment.

FIGURES

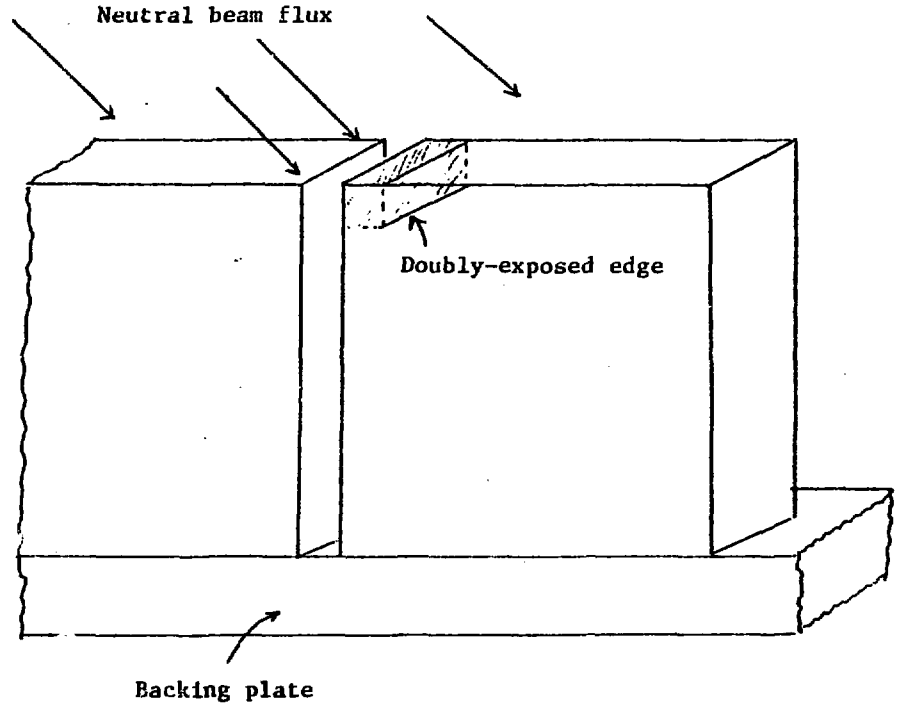

FIGURE 1

Cube-on-plate design, showing region of greater exposure to heat flux.

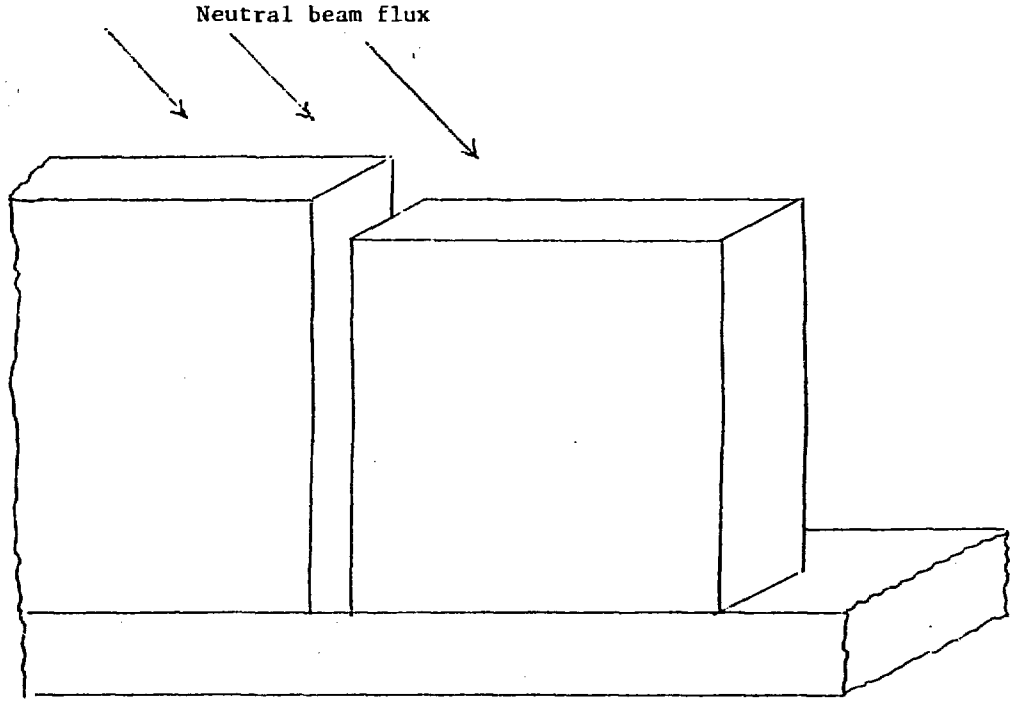

FIGURE 2

Cube-on-plate design which avoids the region of greater exposure to heat flux.

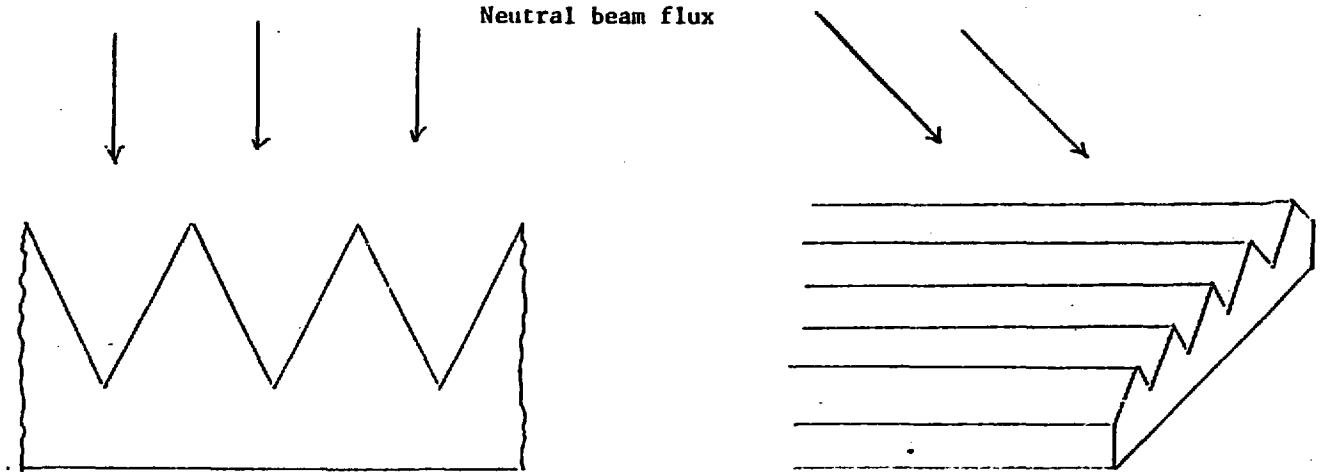

FIGURE 3

Wedged surface design.

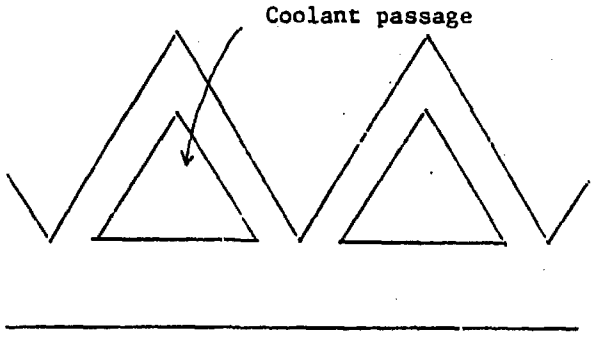

FIGURE 4

Wedged surface design with internal cooling.

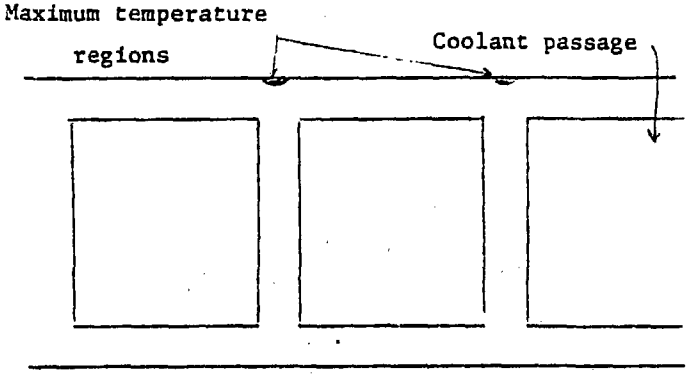

FIGURE 5

Internally-cooled rectangular ducts.

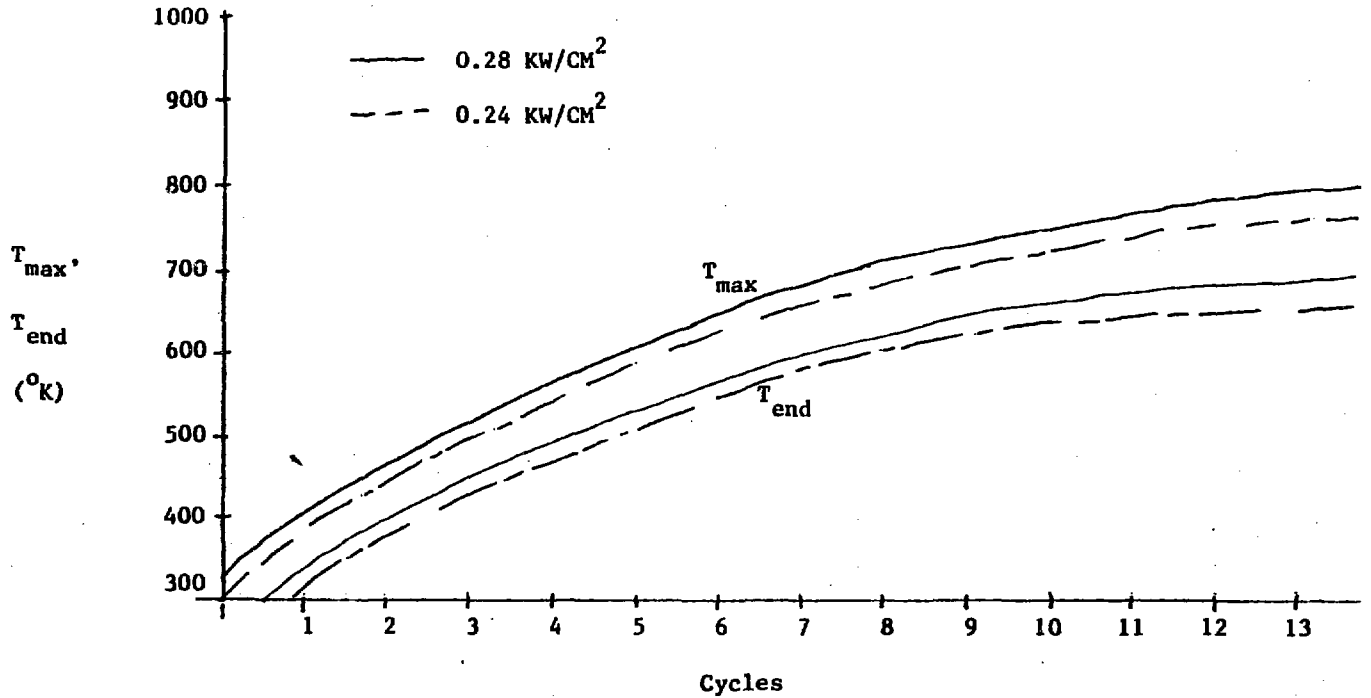

FIGURE 6a

Effect of series of attenuated neutral beam pulses on the temperature of a tungsten plate.

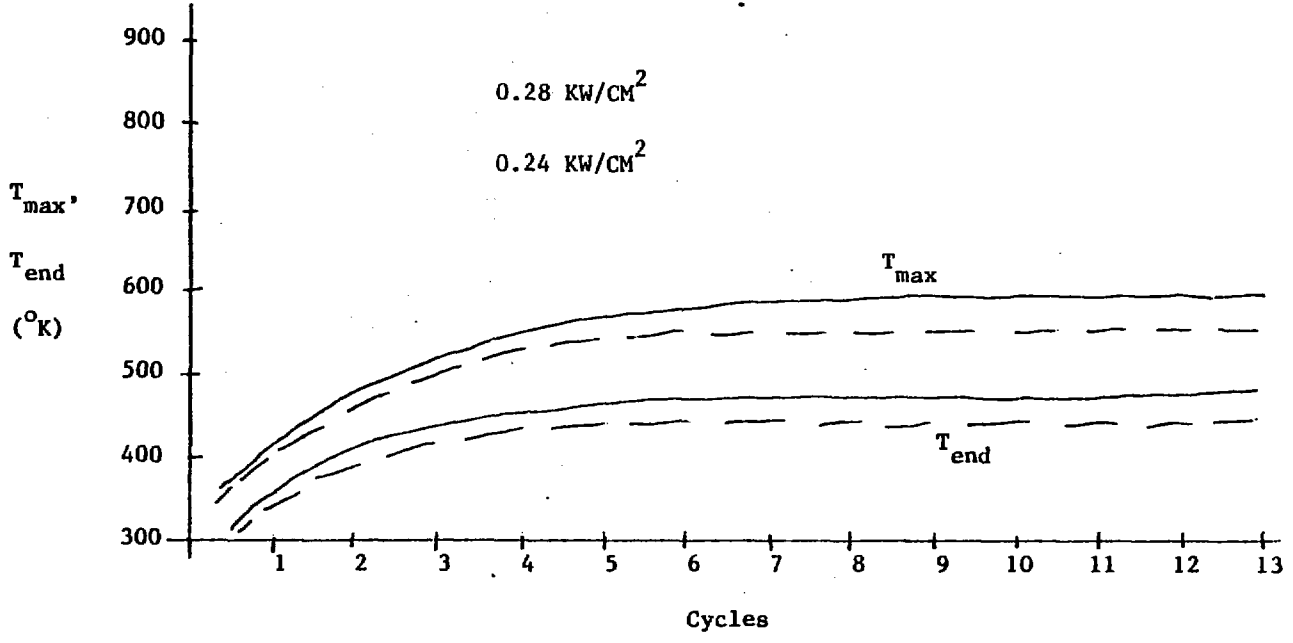

FIGURE 6b

Effect of series of attenuated neutral beam pulses on the temperature of a graphite plate.

FIGURE 7A Maximum allowable heat flux vs. pulse time for a tungsten plate.

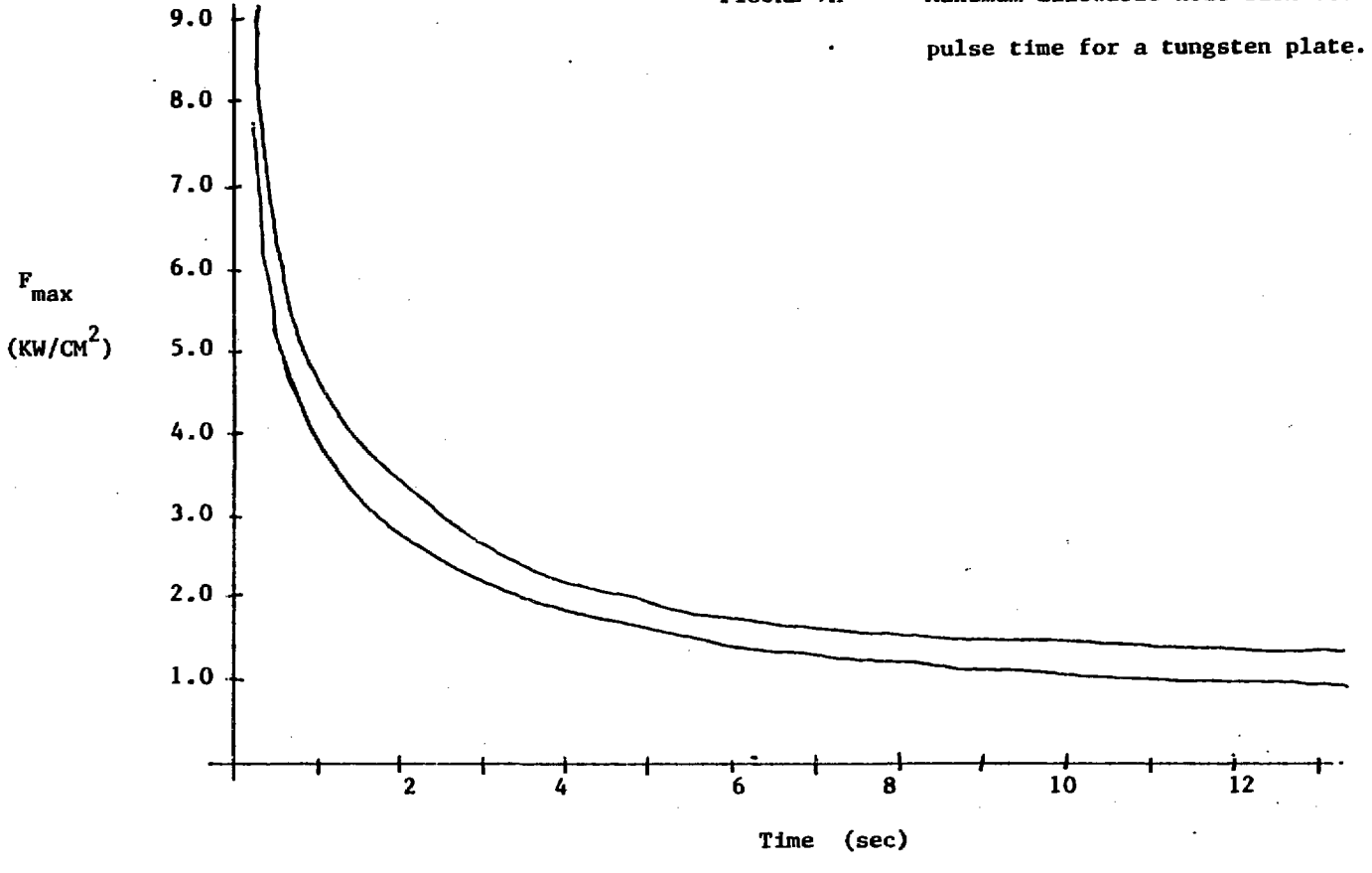

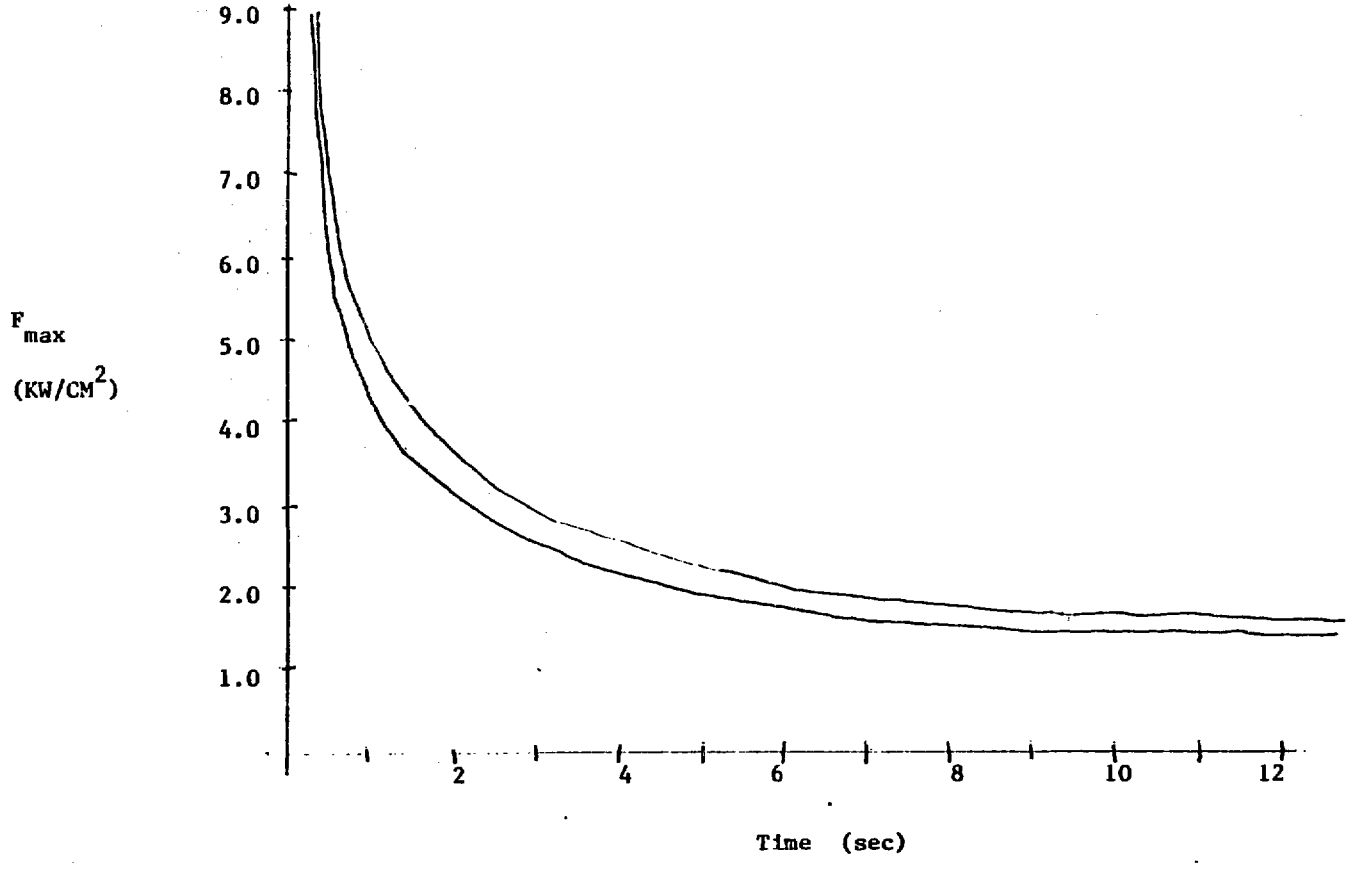

FIGURE 7b. Maximum allowable heat flux vs. pulse time for a graphite plate.

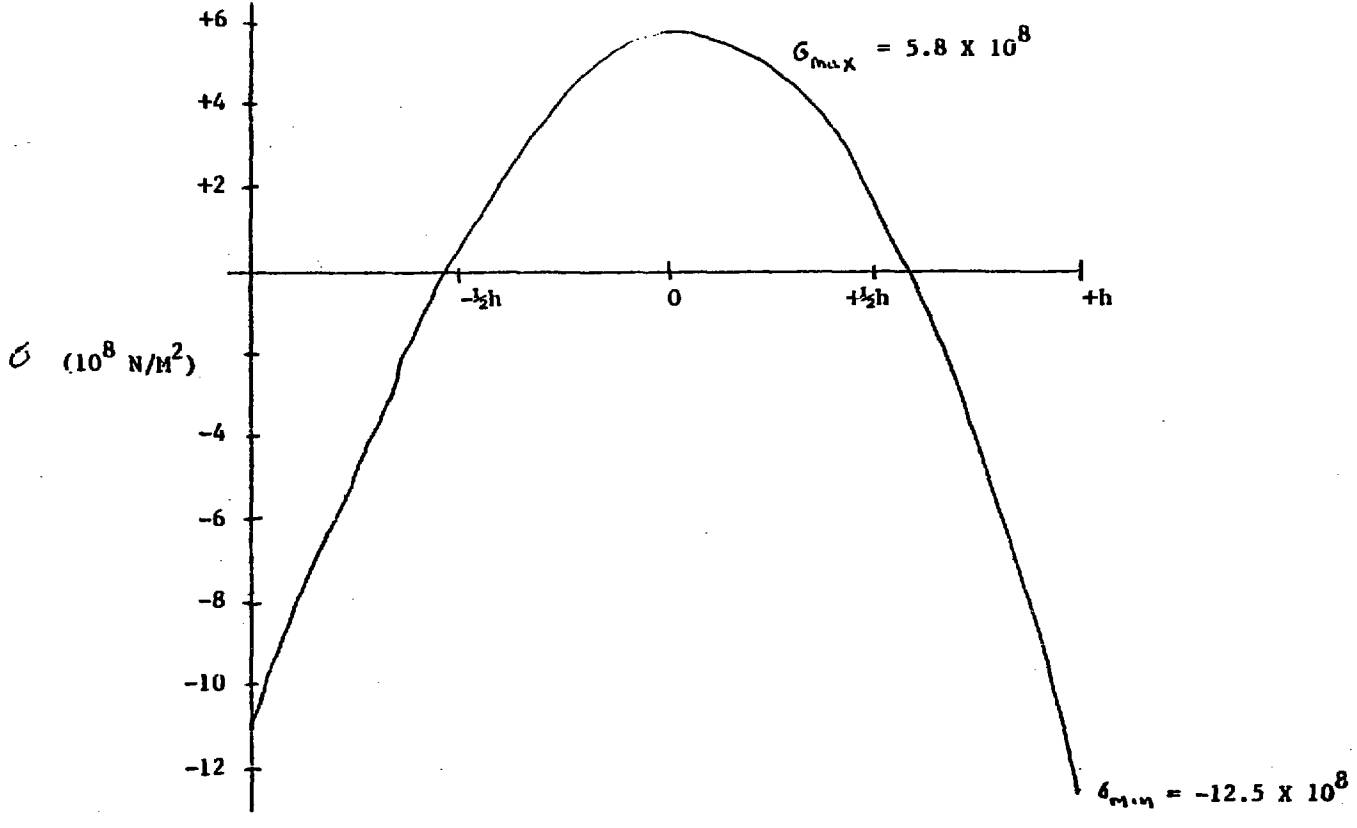

FIGURE 8a

Thermal stress vs. thickness under unattenuated flux on tungsten plate. F= 5.5 KW/CM^2

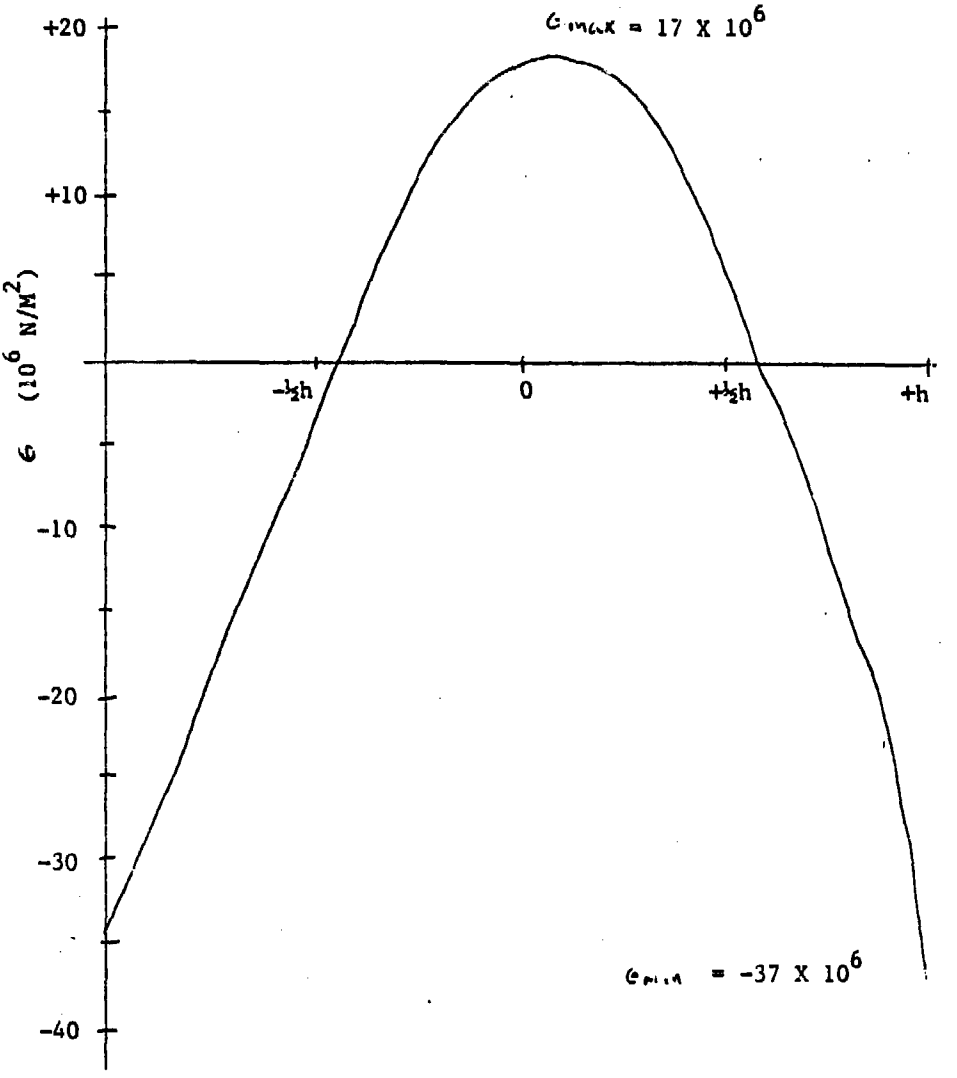

FIGURE 8b

Thermal stress vs. thickness for attenauted flux on tungsten plate

F= 0.22 KW/CM^2

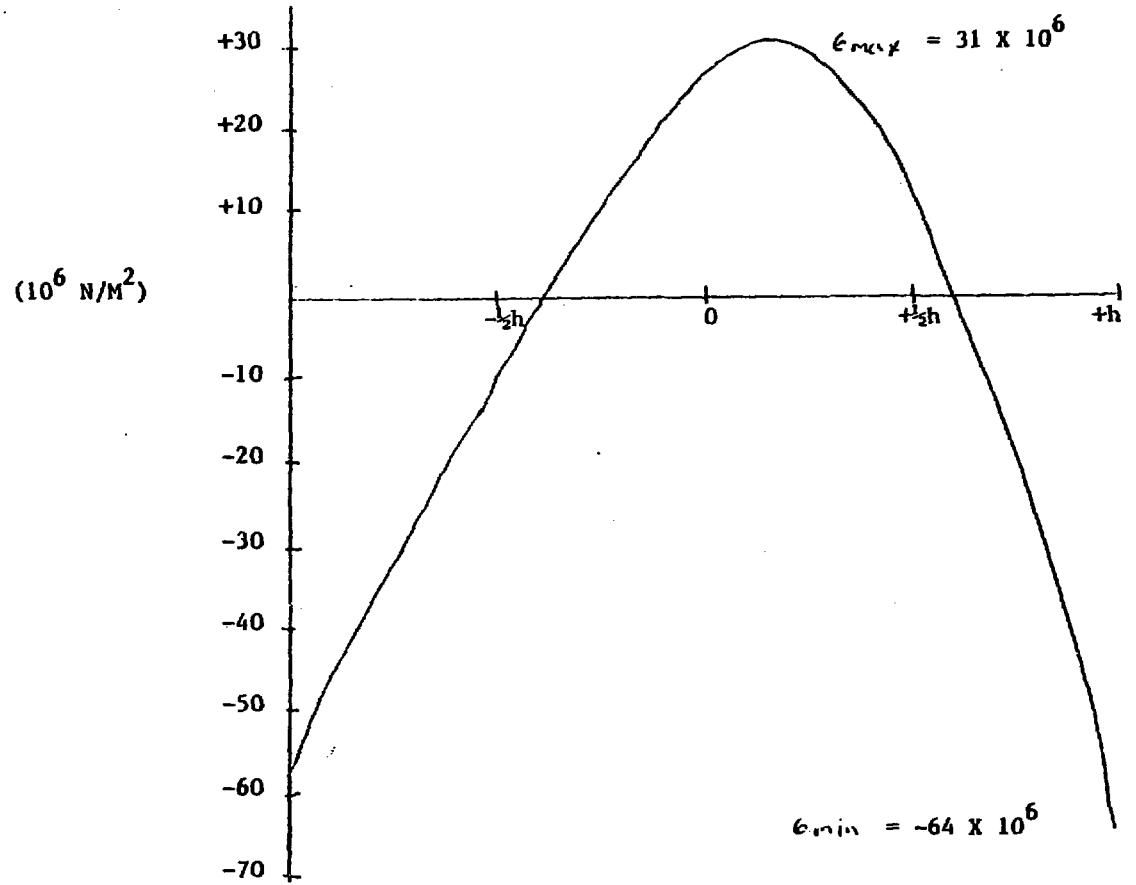

FIGURE 8c Thermal stress vs. thickness for unattenuated flux on graphite plate. F= 6.5 KW/CM^2

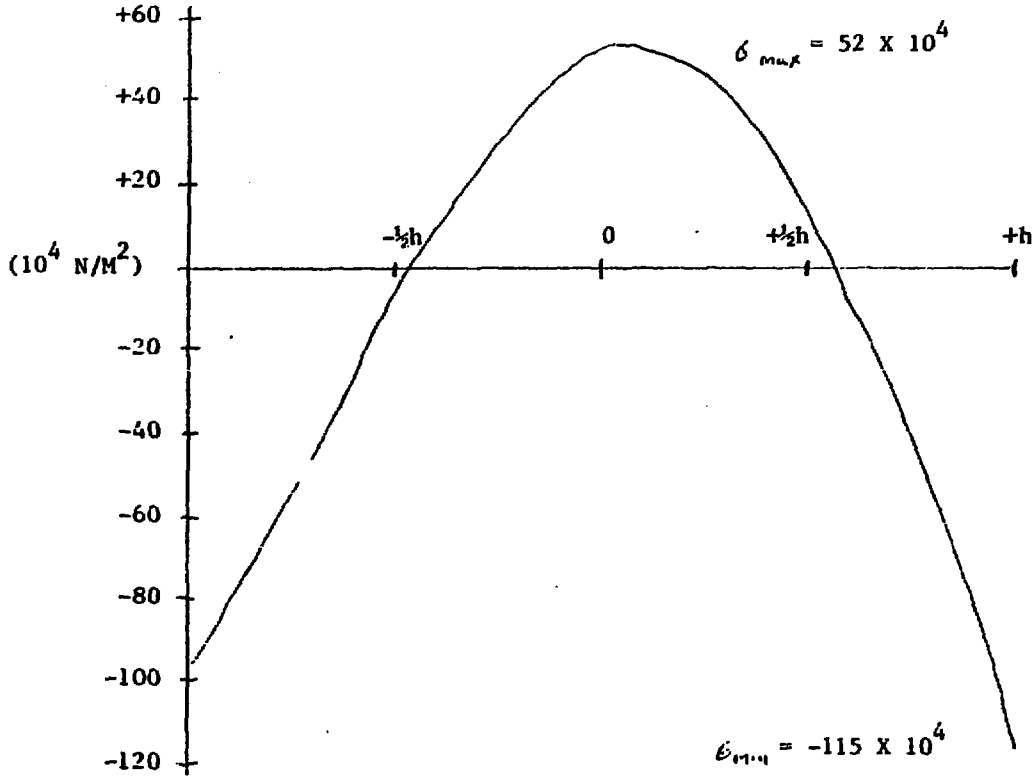

FIGURE 8d Thermal stress vs. thickness for attenuated flux on graphite plate. F= 0.26 KW/CM^2

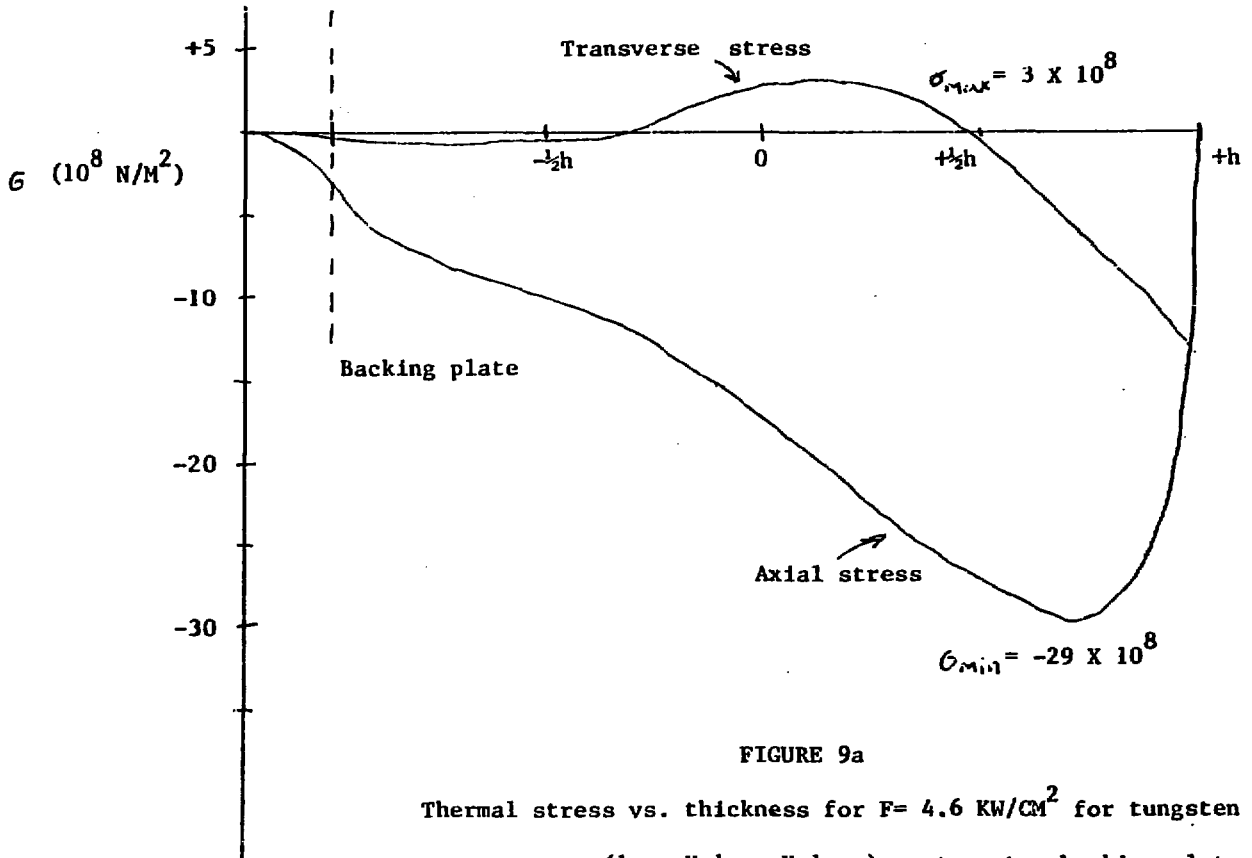

FIGURE 9a

Thermal stress vs. thickness for F= 4.6 KW/CM^2 for tungsten cube (1 cm X 1 cm X 1 cm) on tungsten backing plate.

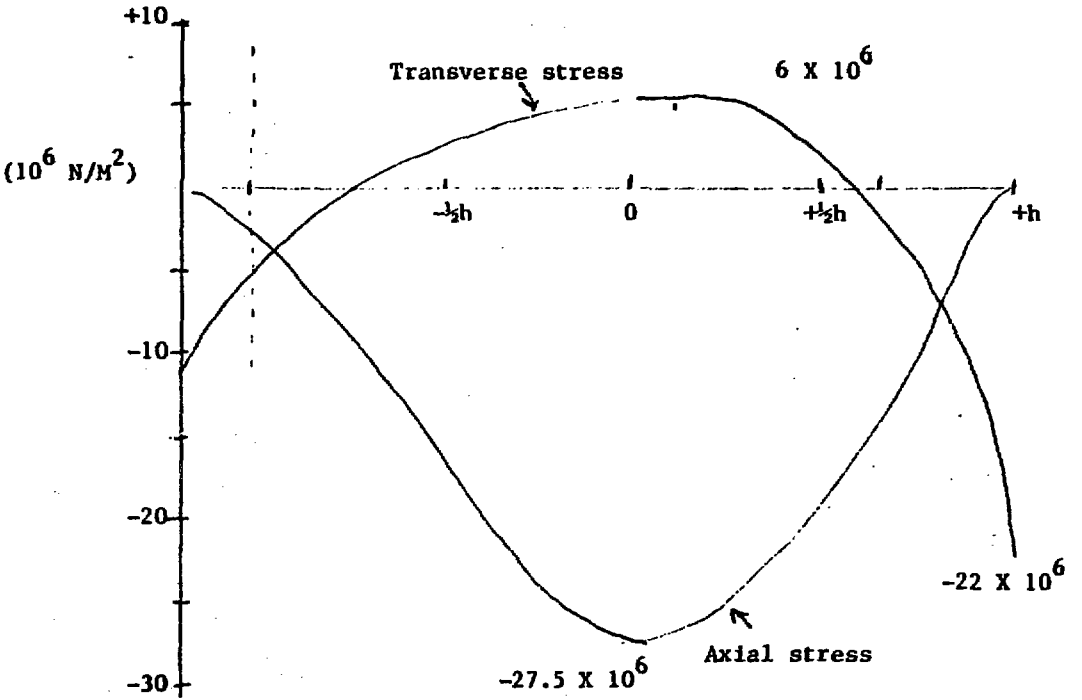

FIGURE 9b

Thermal stress for F= 0.184 KW/CM^2 on tungsten cube (1 cm X 1 cm X 1 cm) on tungsten backing plate.

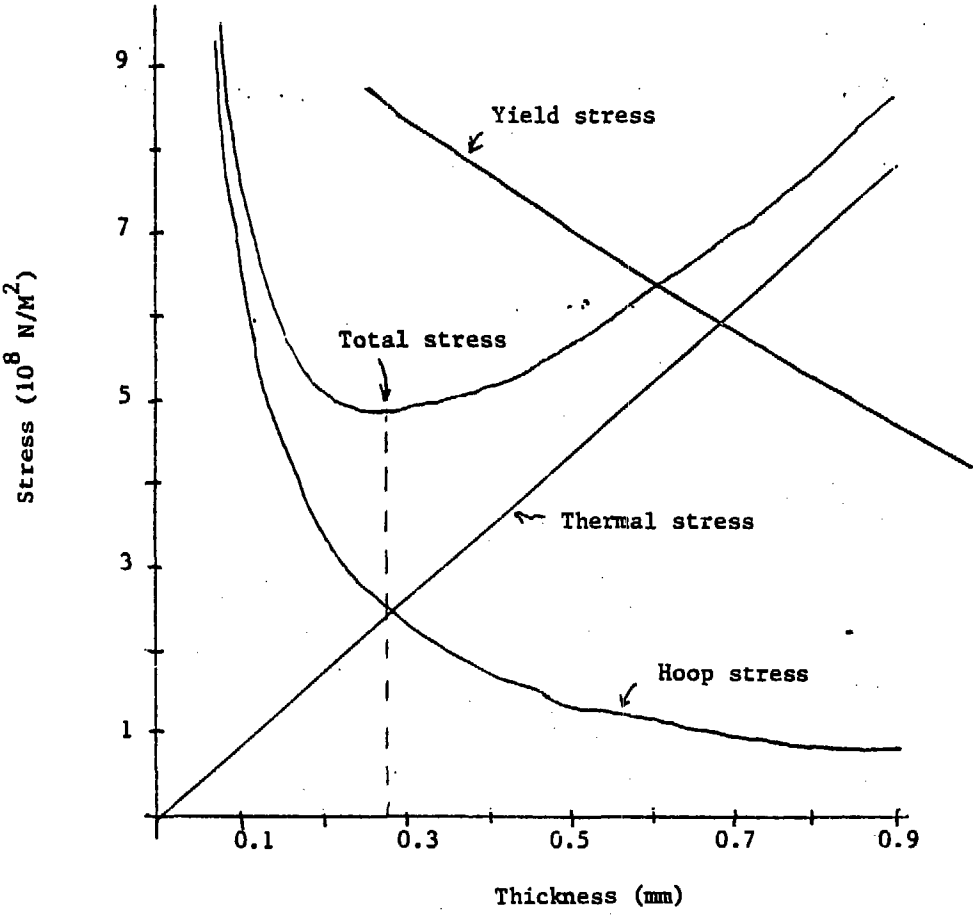

FIGURE 10

Stresses in tungsten tube. D= 10 mm, p= 2000 psi, F= 7 KW/CM^2

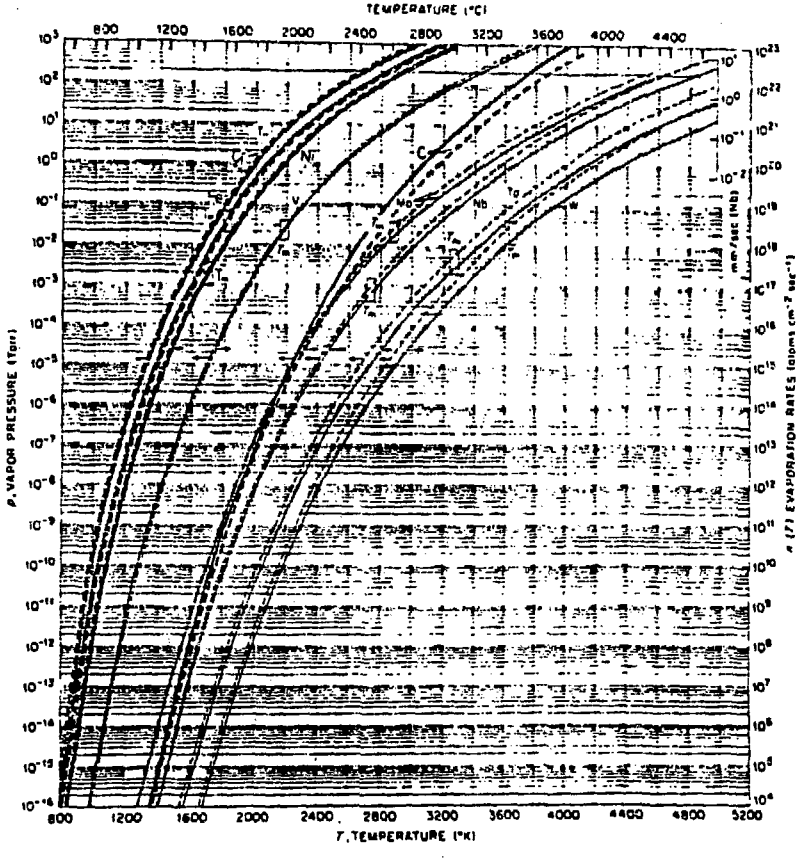

FIGURE 11. Vapor pressures and evaporation rates for different first wall materials.[24]

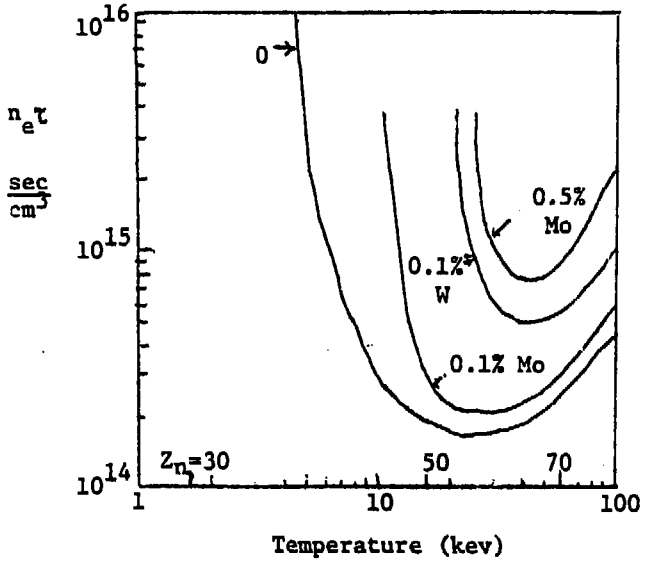

FIGURE 12. The ignition condition for a D-T reactor with various concentrations of high-Z molybdenum and tungsten impurities. The vertical bars indicate the temperature at which the ions of nuclear charge Z_n are ionized to helium-like states.[25]

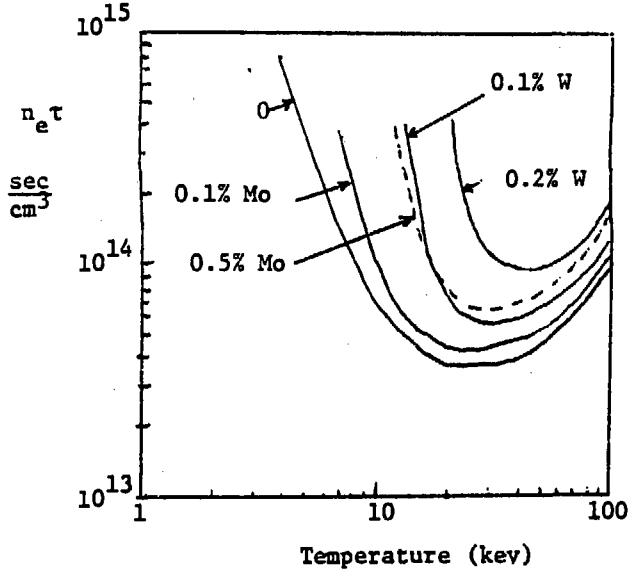

FIGURE 13. The Lawson Condition for a D-T reactor with various high-Z impurity concentrations.[25]

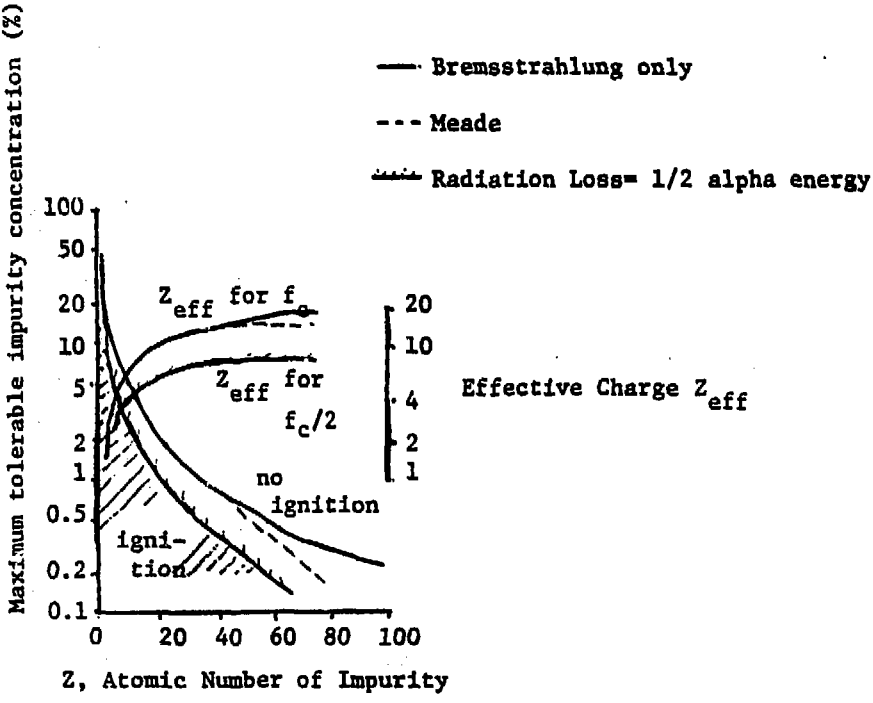

FIGURE 14. Critical impurity concentrations and the corresponding Z_{eff} for a D-T fusion plasma.[24]

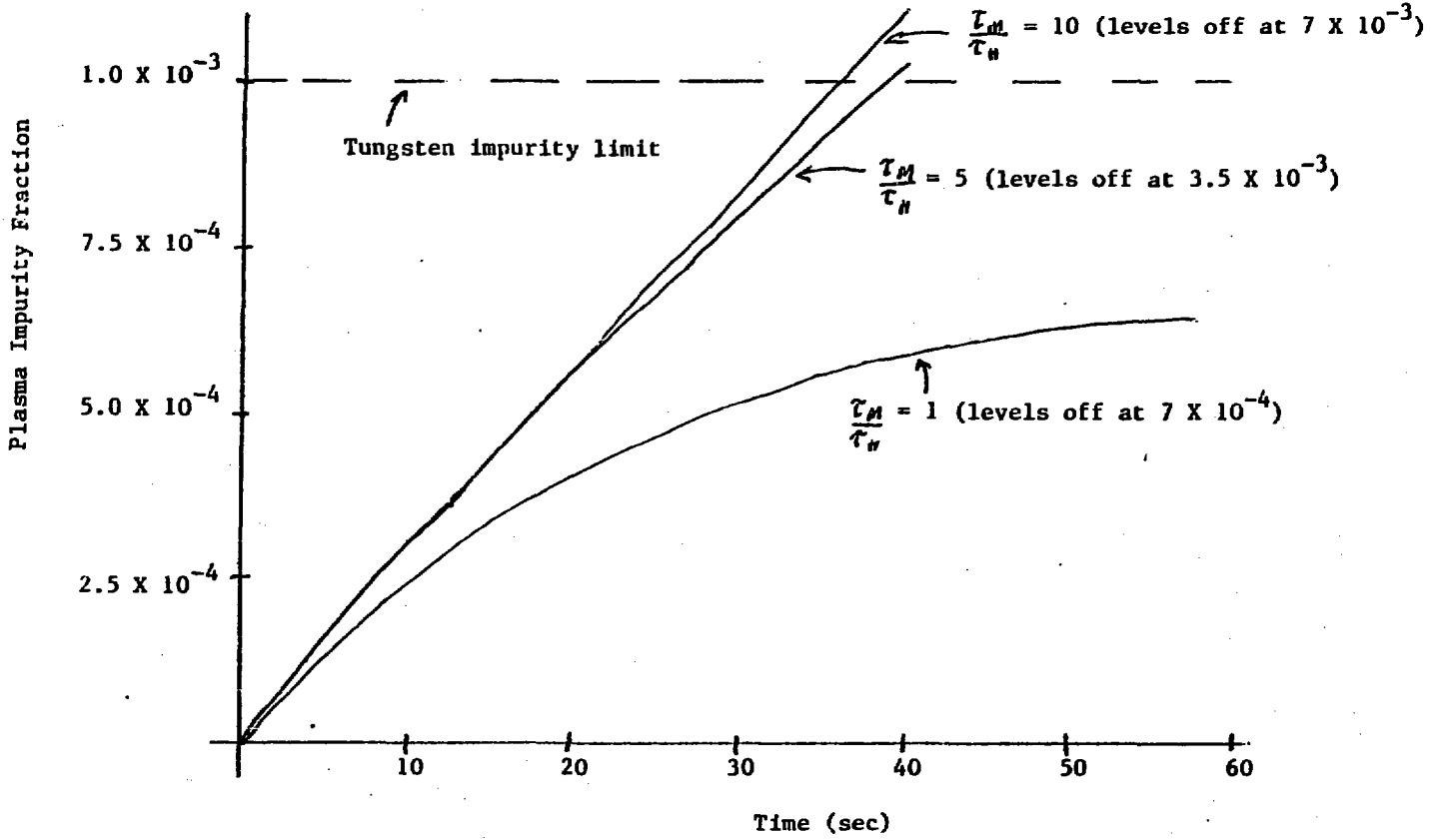

FIGURE 15 Tungsten plasma impurity fraction vs. time for a fusion power reactor.

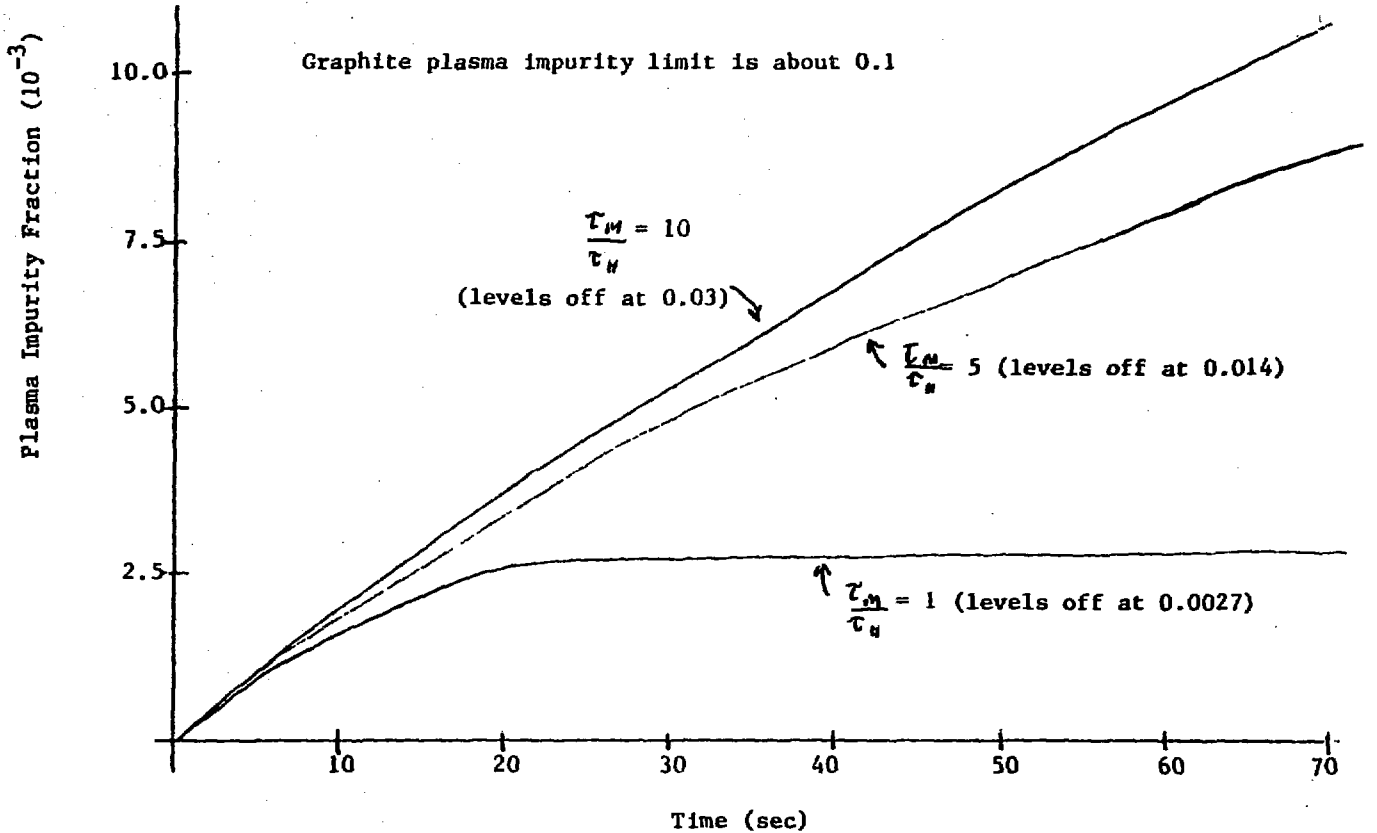

FIGURE 16 Graphite plasma impurity fraction vs. time for a fusion power reactor.

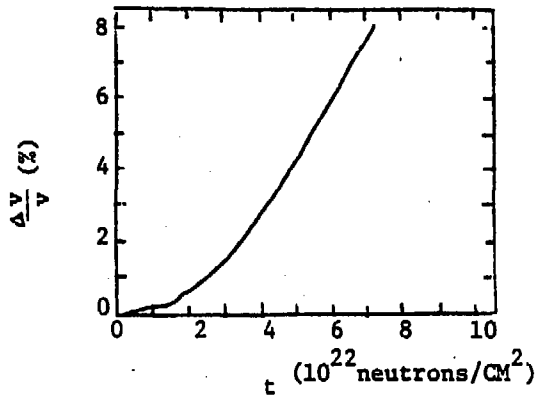

FIGURE 17.
Void-induced swelling in 304 stainless steel at 480°C as a function of neutron fluence.[43]

FIGURE 18. Thermal conductivity changes of graphite measured at the irradiation temperature.[49]

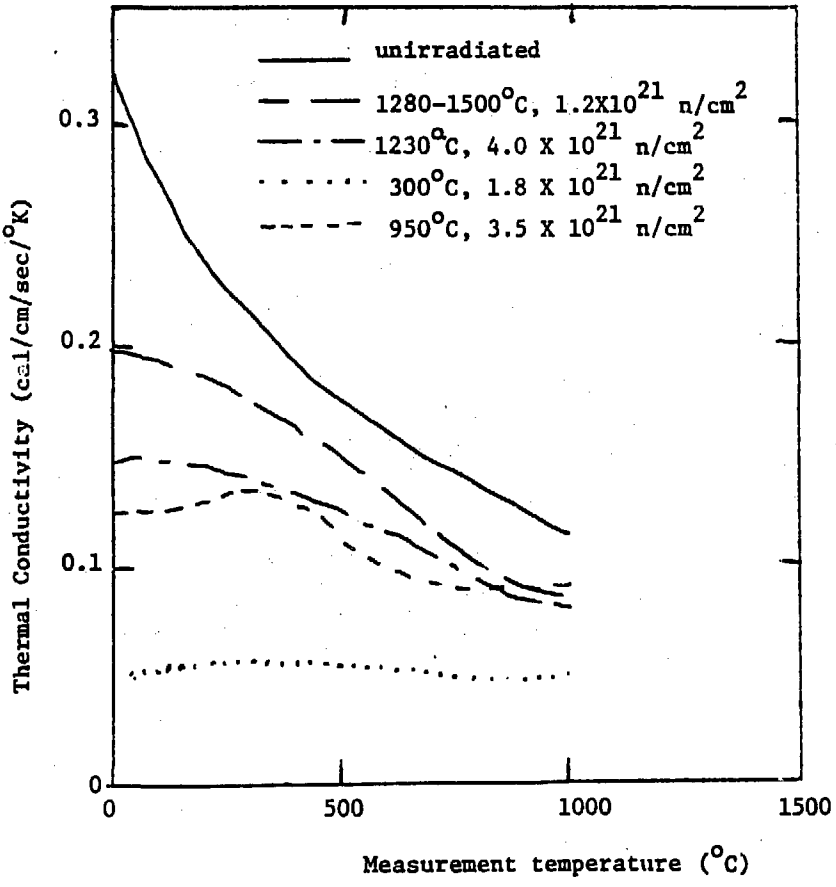

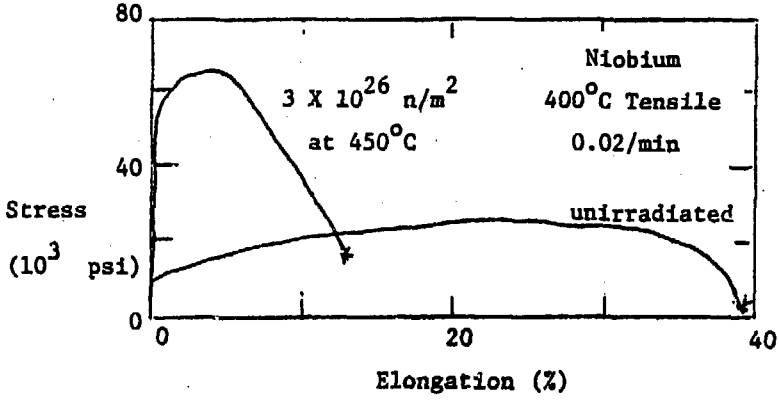

FIGURE 19. Ductility loss by hardening in neutron irradiated niobium. Irradiation in EBR-II to 3 X 10^{22} n/cm^2 at 450°C. [45]

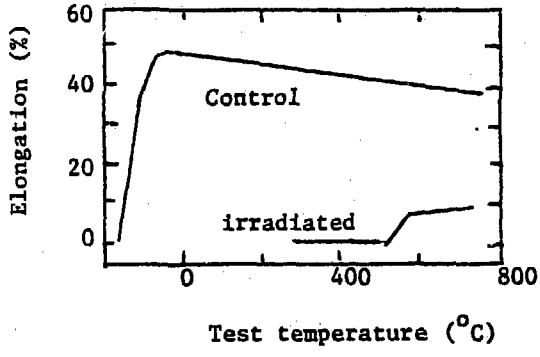

FIGURE 20. Total tensile elongation as a function of test temperature for molybdenum. [43]

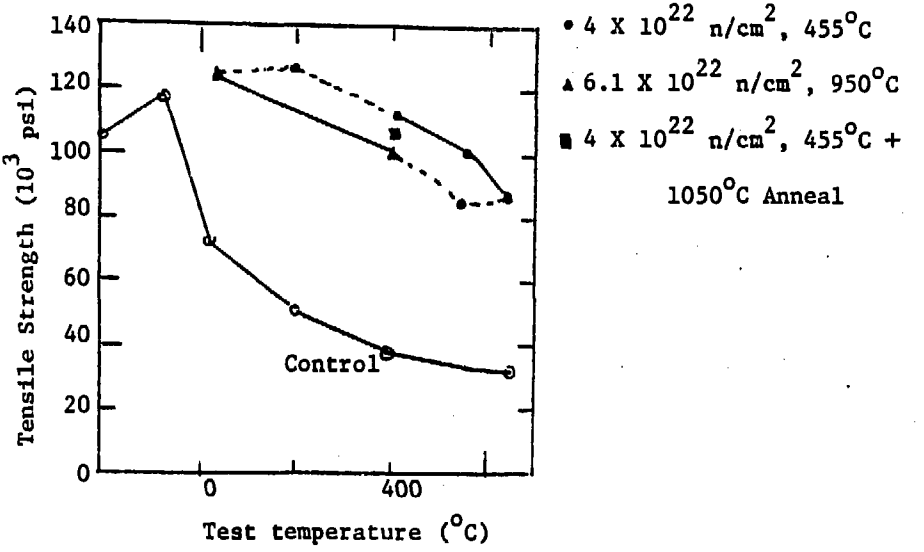

FIGURE 21. The ultimate tensile strength for irradiated and control samples of molybdenum. Dashed lines connect results where irradiation conditions or strain rates are not held costant. Solid lines connect results that differ only in test temperature.[45]

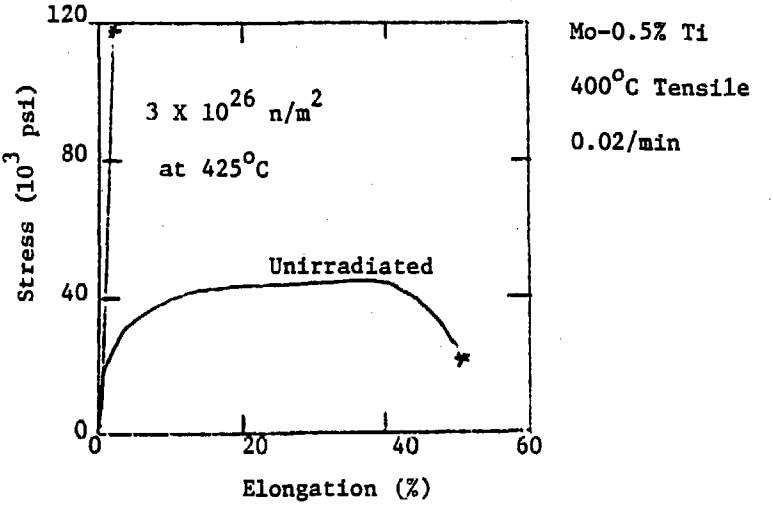

FIGURE 22a. Brittle fracture produced in Mo-0.5% Ti by neutron irradiation. Irradiation in EBR-II to 3 X 10^{22} n/cm^2 at 425°C.[45]

FIGURE 22b. Effect of neutron irradiation (5×10^{19} n/cm^2) on tensile properties.[12]

Temperature (°C)	Yield Point (kg/mm^2)		Tensile Strength (kg/mm^2)		Relative Elongation (%)	
	Before Irradia.	After Irradia.	Before Irradia.	After Irradia.	Before Irradia.	After Irradia.
20	65.5	69.5	69.8	73.0	23.6	22
90	56.2	65.2	63.3	65.4	23.8	18.4
200	49.2	59.8	52.3	60.1	2.8	5.8

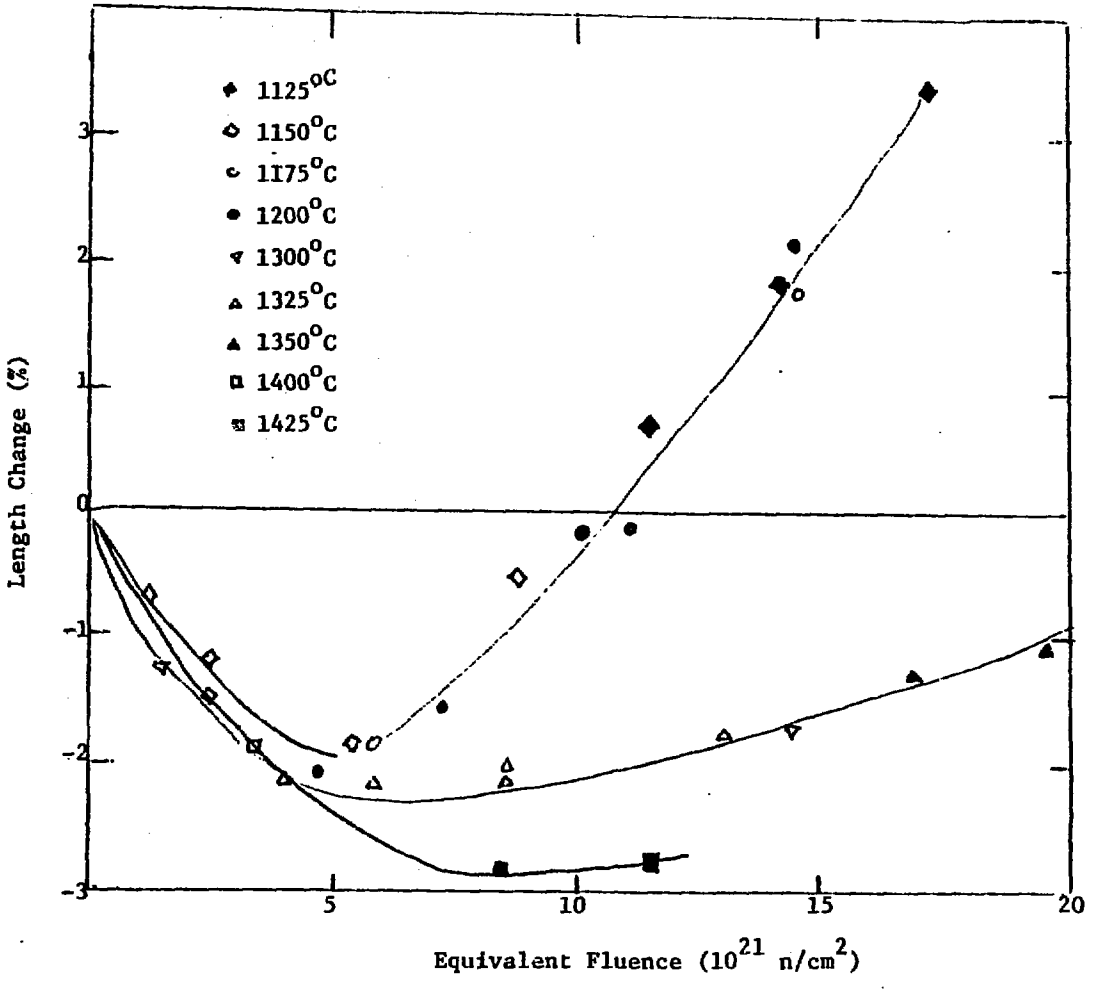

FIGURE 23.

Swelling of graphite due to neutron irradiation.[49]

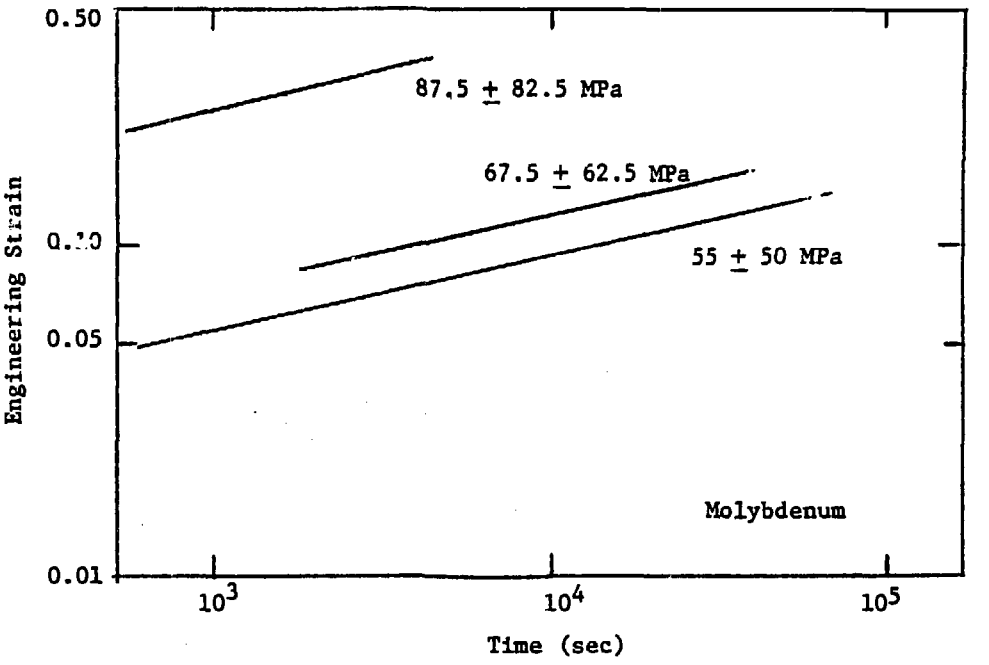

FIGURE 24. The strain-time relationship for various cyclic stress levels at 1153°K. The stress levels indicate the media stress and the extremes.[42]

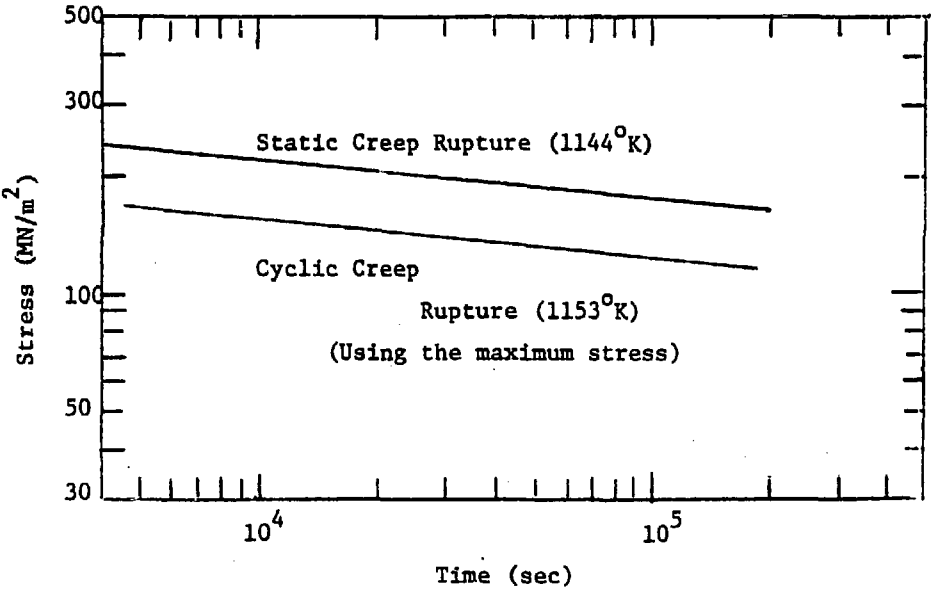

FIGURE 25. The time to failure under cyclic stressing as a function of stress at 1153^{o}K. A static rupture case is included for comparison.[42]

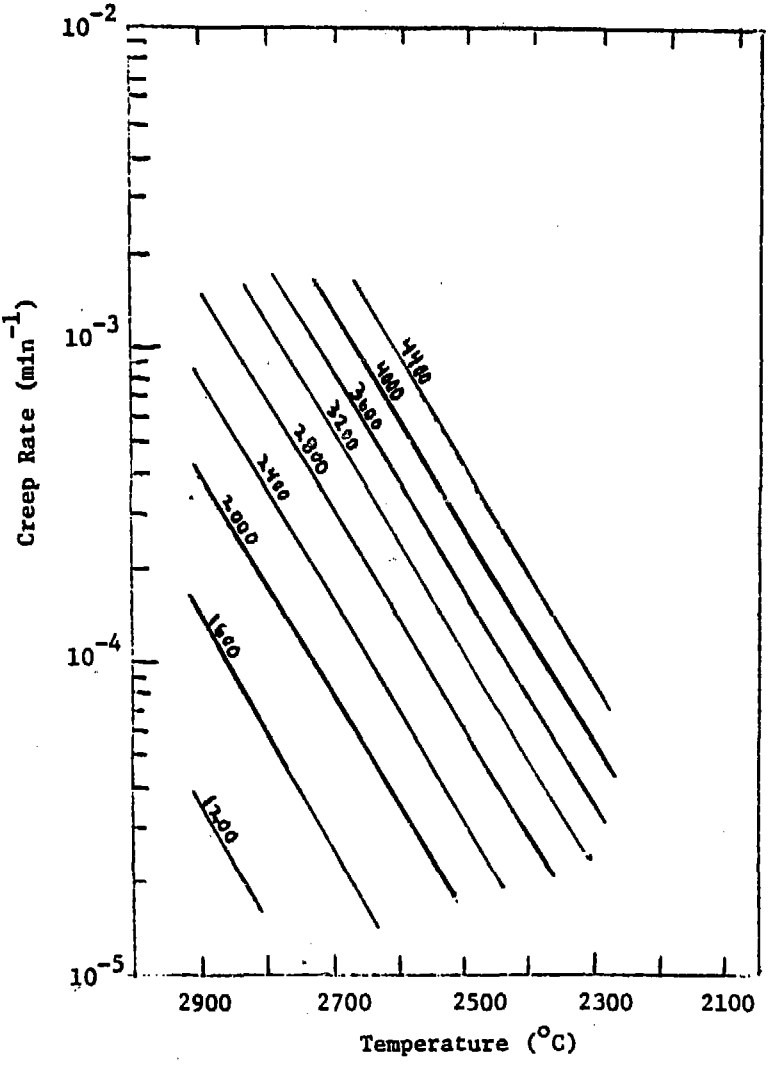

FIGURE 26. Tensile creep of ATJ Graphite oriented with the grain.

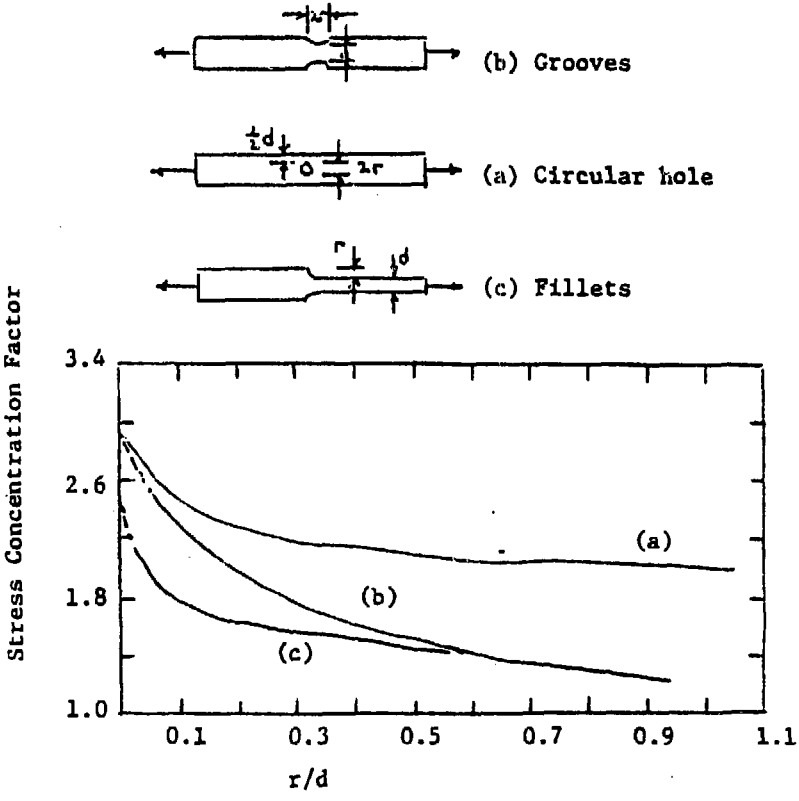

FIGURE 27. Stress concentration for flat plates.